

Performance Analysis of Hybrid-Electric Propulsion Systems for Regional Commuter Aircraft

GUSTAVO MULLER HAUCK

Aeronautics Institute of Technology (ITA), São José dos Campos, São Paulo, Brazil

CLEVERSON BRINGHENTI

Aeronautics Institute of Technology (ITA), São José dos Campos, São Paulo, Brazil

MAURICIO ANDRÉS VARELA MORALES

Flight Mechanics Department, Embraer S.A., São José dos Campos, São Paulo, Brazil

JESUINO TAKACHI TOMITA

Texas A&M University – Department of Aerospace Engineering, TX College Station, United States of America

ANTONIO BRUNO DE VASCONCELOS LEITAO

Aeronautics Institute of Technology (ITA), São José dos Campos, São Paulo, Brazil

FRANCO JEFFERDS DOS SANTOS SILVA

Aeronautics Institute of Technology (ITA), São José dos Campos, São Paulo, Brazil

KONSTANTINOS KYPRIANIDIS

Mälardalen University, Västerås, Sweden

Abstract—Aviation plays a fundamental and valuable role in the modern world, yet it faces significant challenges, including high fuel costs and substantial environmental pollution. These issues have prompted the aviation industry to establish emission standards and develop less-polluting propulsion systems, such as those utilizing synthetic fuels, fuel cells, and electrification. Among these, electrification holds promise as a potential solution for reducing emissions in commuter aircraft, despite the mass limitations posed by batteries. In this study, a methodology was developed and implemented within in-house software to simulate the performance of a commuter aircraft with a hybrid-electric propulsion system. The analysis focused on key metrics like fuel economy and climb time to cruise altitude. The EMB-120 Brasília was chosen as the base aircraft for this research.

Its long-standing use by the Brazilian Air Force (FAB), the authors' extensive familiarity with its performance, and the availability of experimental data for lift and drag coefficients made it an ideal model for our simulations. To evaluate the performance of the hybrid propulsion system and compare it with the standard case, a gas turbine was utilized as the primary engine. Mathematical models were developed for the PW118 gas turbine, which powers the real aircraft that was considered the standard case, and for the PT6A-68C, which was suggested as a substitute for the hybrid system. To evaluate the aircraft's performance, a standard mission was simulated on a short-range route of 926 km (500 NM), flying at an altitude of 7,620 m (25,000 ft), a common mission that is used by Brazilian Air Force. For hybrid simulations, battery packs were tested with specific energies ranging from 0.125 kWh/kg to 0.750 kWh/kg, in multiples of the initial value. Batteries with 0.250 kWh/kg were considered the current state-of-the-art, while the 0.750 kWh/kg packs represent an extreme upper bound associated with far-future technological developments. The results demonstrated significant performance gains depending on the chosen battery technology and the power split, the hybrid system achieved fuel savings of up to 18 % to 19 % and reduced climb time by 17 % to 25 %.

Keywords: Propulsion; Hybrid-Electric Propulsion; Gas Turbine; Aircraft Performance.

Nomenclature

b	=	Wing Span
c	=	Fuel Consumption Factor
C_D	=	Dimensionless Drag Coefficient
C_{D0}	=	Zero-Lift Drag Coefficient
C_L	=	Dimensionless Lift Coefficient
C_{L0}	=	Empirically Obtained Coefficient for C_L
$C_{L\alpha}$	=	Lift Gradient
e	=	Oswald Efficiency Factor
P_{EM}	=	Electric Motor Power
P_{Shaft}	=	Total Shaft Power
S	=	Power Split
S_W	=	Wing Surface Area
t	=	Instant Time
V_{climb}	=	Climb Rate
$V_{descent}$	=	Descent Rate
α	=	Angle of Attack (AoA)
γ	=	Flight Path Angle
η_{batt}	=	Battery-Set Efficiency
η_{cab}	=	Cable-Set Efficiency

η_{coup}	=	Mechanical Coupling Efficiency
η_{EM}	=	Electric Motor Efficiency
$\eta_{\text{elec syst}}$	=	Electric System Efficiency
η_{inv}	=	Inverter Efficiency
η_{prop}	=	Propeller Efficiency

Manuscript received XXXXX 00, 0000; revised XXXXX 00, 0000; accepted XXXXX 00, 0000.

Authors' addresses: Gustavo Muller Hauck, Cleverson Bringham, Jesuino Takachi Tomita (currently in the Department of Aerospace Engineering, Texas A&M University), Antonio Bruno de Vasconcelos Leitao and Franco Jefferds dos Santos Silva are with the Department of Turbomachines, Aeronautics Institute of Technology (ITA), São José dos Campos, São Paulo, 12228-900, Brazil, E-mail: (gustavomhauck@gmail.com; cleverson@ita.br; jtakachi@tam.u.edu; antoniobruno@ita.br; jefferds@ita.br); Mauricio Andrés Varela Morales is with the Flight Mechanics Department, Embraer S.A., São José dos Campos, São Paulo, 12227-901, Brazil, E-mail: (morales@ita.br); Konstantinos Kyprianidis is with School of Business, Society and Engineering, Mälardalen University, 883, SE-72123 Västerås, Sweden, E-mail: (konstantinos.kyprianidis@mdu.se). (Corresponding author: Cleverson Bringham.)

I. INTRODUCTION

Aviation, an invention of the early 20th century, has revolutionized how humanity travels and transports goods. In 2019, global aviation transported 4.5 billion people. Before the Covid-19 pandemic, it was already responsible for 87.7 million direct and indirect jobs, with 11.3 million people employed in manufacturing and other industrial sectors. While air transport accounts for only 0.5 % of the total volume of worldwide shipments, it represents 35 % of the value of global transactions [1]. This is due to its role in moving high-value cargo or goods with special requirements, such as speed.

Like the aircraft itself, the technology in this area has evolved rapidly. In the 1960s, aviation was a wasteful and loud means of transportation [2], but today it is up to 80 % more fuel-efficient per seat-kilometer. Despite this progress, flights were responsible for emitting 915 million tons of carbon dioxide (CO₂) into the atmosphere in 2019, according to the Air Transport Action Group (ATAG). About 98 % of aviation's CO₂ emissions come from aircraft with a gross takeoff mass over 25 metric tons. More than 50 % of these emissions are from twin-aisle aircraft flying distances greater than 6,500 km, while only 12 % are produced by flights with a range of less than 750 km [3]. Currently, aviation is responsible for 2 % of all human-generated CO₂. However, it is important to note that global air traffic has nearly doubled every 15 years since 1970. If this trend continues, approximately 10 % of

all human CO₂ emissions will come from aerial activities by 2035 [4].

In the current context of social and environmental responsibility, reducing aviation's carbon footprint is of fundamental importance. This goal directly impacts the economics of airlines and aviation operators, which typically operate on very thin profit margins. In 2019, fuel accounted for 23.7 % of airline costs [1], with single-aisle aircraft consuming 50 % of all commercial aviation fuel in the U.S. [5].

With the necessity to reduce emissions in mind, numerous studies have been published investigating the possibility of adding electric systems to, or substituting existing ones in, aircraft. This context highlights the opportunity to explore propulsion systems that also rely on electric motors. Furthermore, battery-powered aircraft can increase energy transfer efficiency from the current propulsion systems' thermal efficiency of approximately 25% to 30% (as is typical for small to medium turboprops) to values higher than 70% [6].

Different studies also explore full-electric aircraft and their energy sources. For example, Barufaldi et al. [7] investigated the fuel consumption of an electric airplane powered by fuel cells. While full-electric aircraft have been designed and built, they are not yet promising for large airplanes and long-range transportation due to battery capacity constraints. In the broader context of transportation, Wang's et. al. [8] presents a high-efficiency dual DC-DC conversion system for long-range submarine vehicles. This system is powered by a combination of fuel cells and batteries. The study details the development and validation of a system that integrates a main converter for high power and an auxiliary one for tracking the fuel cell's maximum power point, thereby optimizing energy conversion efficiency.

The current limitations in battery technology, specifically in terms of specific energy and specific power, are a major factor. These limitations necessitate a significant increase in mass, which is a major constraint for aeronautical applications. As a result, it makes sense to explore the possibilities of fuel and overall energy savings, as well as emission reductions offered by hybrid-electric propulsion systems. These systems combine conventional gas turbine components with electrical elements that directly generate thrust. In addition to the economic benefits of cheaper operations due to reduced fossil fuel consumption, hybrid technology also has the potential to optimize critical flight phases and extend the range of aircraft into distant regions without heavy logistical support.

Recent studies on hybrid-electric propulsion systems suggest that fuel savings of up to 22 % [9] and 28 % [10] may be achieved. These values vary significantly between

studies, largely due to a lack of consolidated principles in this developing field. For example, Sielemann et al. [11] report that for regional aircraft, fuel economy has been found to range from 30 % to minimal benefit. This discrepancy is a result of various factors, including different considerations in component modeling (using masses, efficiencies, and physics-based electric models). A common approach to internal combustion engines, in combination with electric assistance, is observed, however: downsizing the core. This can be achieved conventionally, by exploring power-specific fuel consumption, or through constant power scaling [11].

Bills et al. [12] investigated the performance requirements of next-generation batteries necessary for the electrification of commercial aircraft. This is a crucial step toward reducing emissions from the air transport sector. The study evaluated the specific power and specific energy requirements for various classes of aircraft, including regional, single-aisle, and wide-body models. It concluded that smaller, shorter-range aircraft have less demanding battery needs, making them more suitable for initial electrification efforts. The research also explored the limitations of both current and future battery technologies, such as lithium-ion and lithium-air, in relation to these requirements. The authors found that advanced chemical batteries are the only technology capable of meeting the demands for electrifying larger commercial aircraft. However, they also suggested that hybrid aircraft could serve as a viable short-term solution to bridge the gap until more advanced battery technologies are fully developed.

A major challenge for electric aircraft propulsion is the low specific energy of current battery technology compared to fossil fuels. Due to this limitation, some analysts suggest that all-electric flight could be restricted to a range of just 50 to 200 miles. Furthermore, some estimates indicate that an aircraft with full electric propulsion would require a battery system weighing 1.7 to 3.8 times the normal maximum take-off mass [13]. Current battery cells are capable of a specific energy of 100–200 Wh/kg, whereas aviation kerosene has an energy density of 12,000 Wh/kg [9]. This stark contrast in energy storage is a primary barrier. For example, a study on a small hybrid aircraft, like a Cessna 172, found that one kilogram of fossil fuel provides the same propulsive energy as ten kilograms of batteries, even with a relatively high specific energy of approximately 400 Wh/kg [14].

Promising technologies, such as lithium-air batteries, could potentially overcome the limitations of current energy storage systems. Research suggests these batteries have a theoretical energy density of 11,680 Wh/kg, but they are not yet ready for operational use [9]. Other metal-air batteries are also being researched, including

aluminum-air (8,140 Wh/kg) and iron-air (14,730 Wh/kg) [15].

Despite the high theoretical values, lithium-air batteries face several challenges. A study by Adu-Gyamfi and Good [16] notes that they have low electrical efficiency (ranging from 60 % to 70 %), poor specific power, and low discharge rates. The authors suggest that for lithium-air batteries to become a viable option, they would need to achieve a specific energy of at least 400 Wh/kg [16]. This minimum requirement is consistent with another research; Nasoulis et al. [17] studied a commuter aircraft and concluded that 500 Wh/kg at the pack level is the minimum specific energy needed to justify electrification. It is crucial to distinguish these system-level requirements from cell-level metrics. The transition from cell to pack involves a cell-to-pack mass factor, which typically ranges from 0.60 to 0.70. This indicates that a completed battery pack retains only about 60% to 70% of the individual cell's specific energy due to the added mass of the Battery Management System (BMS), thermal management, and structural enclosures [18]. In contrast, Kozakiewicz and Grzegorzczak [6] predict that current lithium-ion batteries could reach 400 to 450 Wh/kg at the cell level in the near future. Consequently, an all-electric propulsion system is currently only feasible for low-mass, short-range aircraft [9]. To estimate the range and endurance of these aircraft, some publications have adapted the traditional Breguet equations [4], [19]. Fredericks et al. [20] highlight the specific battery requirements for e-VTOL (electric vertical take-off and landing) aircraft. These vehicles require not only high specific energy but also very fast discharge rates to support the demanding take-off and landing phases. The study also identifies other critical challenges, such as thermal management and durability, which are essential for the commercial viability of electric urban air mobility.

When considering an aircraft's range and autonomy, it's essential to define the specific mission requirements. Pernet et al. [21] suggest that the regional market presents the most promising option for electrification. Their study showed that using batteries with a specific energy of 1,500 Wh/kg could lead to a 20 % reduction in fuel consumption. However, this benefit came at a high cost, as there was a significant trade-off in payload availability relative to the aircraft's maximum take-off weight [21].

When discussing hybrid and electric aircraft propulsion, the system's architecture is a critical factor. The integration of gas turbines and electric motors can be configured in various ways, each with different advantages. A system is considered hybrid if it includes a battery that can be charged on the ground or in the air by an Internal Combustion Engine (ICE). This ICE may also provide thrust. If the system relies solely on batteries, it is

classified as all-electric. Conversely, a system that uses a GT only to power an electric motor via a generator, without the GT providing thrust or the system using batteries, is called turboelectric. In a series hybrid configuration, the gas turbine drives a generator to supply electrical power, while only the electric motors produce thrust. Conversely, in parallel hybrid configuration, both the gas turbine and the electric motor are mechanically coupled to jointly provide thrust. A detailed description of these architectures and their respective schematics is presented in Section II.B. Current energy storage technology makes all-electric configurations impractical for most applications. However, both partially turboelectric and parallel hybrid systems are considered viable for introduction by 2035 [22]. A study by Nasoulis et al. [23] compared series and parallel hybrid-electric configurations to a conventional reference aircraft. The analysis was based on 400-nautical-mile missions (with an additional 100-nautical-mile diversion), using electric power during take-off, climb, and cruise. The study used batteries with specific energy ranging from 400 to 1,000 Wh/kg. The results indicated that by 2040, parallel hybrid variants could achieve 28 % to 33 % savings in energy and block fuel, respectively. In contrast, series hybrid systems showed significantly better performance, with potential savings of 58 % in energy and 66 % in block fuel. These projections assume a 25 % reduction in gas turbine specific fuel consumption by that same date.

Studies indicate that a parallel hybrid architecture is the most effective configuration for optimizing fuel savings in aviation applications [10]. The power distribution strategy is another key factor to consider. One option is to use electric power throughout the entire flight to supplement the aircraft's propulsion. Voskuil et al. [9] explored this concept by modeling a hybrid-electric system in a parallel architecture for an ATR-72-600 turboprop. This aircraft is typically capable of carrying 70 passengers on 825-nautical-mile missions. The study assumed the use of lithium-air batteries with a specific energy of 750 to 1,500 Wh/kg, which those authors expected to be commercially available by 2035. However, recent assessments indicate that achieving pack-level specific energies of even 500 Wh/kg by 2035 is challenging. Consequently, the 750–1,500 Wh/kg range is currently considered optimistic and more representative of far-future scenarios rather than near-term commercial availability. The research used two distinct approaches for power management: Constant power split, where a fixed percentage of the total power was supplied by the electric system; and constant gas turbine operating regime, where the gas turbine was kept at an operating point, with the electric system providing the rest of the power based on a power loading diagram. The results showed significant potential for fuel savings.

For example, using 1,000 Wh/kg batteries with a constant power split of 34 % electric power throughout the flight resulted in a 28 % fuel saving for the mission. However, this gain came at the cost of a 14 % increase in the maximum take-off mass (MTOM).

A study by Nasoulis et al. [17] applied a parallel-hybrid configuration to a commuter aircraft to analyze its performance. The research found a direct relationship between the degree of hybridization and block fuel reduction when the aircraft's mass remained constant: as the degree of hybridization increased, the reduction in block fuel improved. However, the inverse was true when the battery's specific energy was held constant. In this scenario, greater block fuel reductions were achieved with a lower degree of hybridization. Overall, the study demonstrated that a parallel-hybrid configuration could lead to fuel savings between 16 % and 22 % compared to a conventional reference aircraft. These results were based on battery specific energies of 920 Wh/kg and 1,140 Wh/kg, respectively [17].

One effective strategy for hybrid aircraft is to optimize the gas turbine for a specific flight phase, typically cruise, while using batteries to provide supplemental power during critical, high-demand phases like take-off and climb. This approach allows for a reduction in engine size and overall fuel consumption [5]. A study by Gesell et al. [10] tested two parallel hybrid setups on an ATR 72 aircraft to evaluate this concept. Both setups assumed a battery specific energy of 700 Wh/kg. The first setup, low hybridization, used batteries to provide 10% of the power during take-off and climb. This required adding 300 kg of mass per propulsion unit but resulted in a 5.2% fuel savings over 300-nautical-mile mission. The second setup, high hybridization, increased the electric power contribution to 40% during the same phases, which pushed the aircraft to its maximum take-off weight (MTOW) limit. This configuration yielded significantly higher fuel savings of 21.6%. The researchers simulated the entire flight mission using data on drag, air speed, and thrust to calculate fuel flow, like the method proposed in this work.

Another study by Marien et al. [24] investigated the relationship between flight range and the benefits of hybridization. They found that for short-range missions, the weight penalty of adding electric components offset any fuel savings, as there was not enough time during the electrified phase to recover the weight penalty. As the mission range increased, an optimum point for fuel economy was identified, which was dependent on the battery's specific energy. However, extending the range beyond this optimum point caused the fuel savings to decrease. This happens because the limited electric energy

storage necessitates reducing the use of electric motors and increasing the reliance on the gas turbine's power.

There are many studies in the literature highlighting the importance of hybridization in propulsion system concerning the hybridization degree, configuration of the system, such as parallel or series, and turboelectric with the aim to guarantee safety operation in all phases of the flight, for a given airplane, using less fuel than the standard propulsion system, thus reducing emissions and ensuring safety operations, as related for example, to quote a just a few, by Goeing et al. [25], Kang et al. [26], Sieleman et al. [27], Carpentier et al. [28], Ghelani et al. [29], Vouros et al. [30], Sahoo et al. [31], Engelbrecht et al. [32], Gimenez et al. [33], Boretti and Castelletto [34], Papadopoulos et al. [35], Ghelani et al. [36], Donateo et al. [37], Fanxin et [38], Zhu et al. [39], Del Pizzo et al. [40] and Hakyemez et al. [41].

Some studies are more conceptual in nature, such as the SUGAR (Subsonic Ultra-Green Aircraft) series developed by Boeing. This series included aircraft concepts designed with both current and future technology planned for the 2030s. The designs focused on a 154-seat aircraft with a range of 900 nautical miles. Comparative analysis between turbofan and hybrid engines in the SUGAR concepts showed potential fuel consumption reductions between 25 % and 46 % [19]. This significant finding underscores the importance of an integrated structure-propulsion design for future hybrid aircraft. The concept of holistic design, which treats the aircraft as a single, integrated system rather than a collection of separate components, has been identified as a key solution for meeting future environmental standards. Major initiatives like The European Flightpath 2050 and NASA's Environmentally Responsible Aviation (ERA) N+ series emphasize this approach. These programs call for the integration of various project elements, including electric or hybrid propulsion systems; the airframe; energy storage; power management and control; landing gear; environmental control systems; avionics. By considering these components as a single, interconnected system, designers can achieve the required improvements in emissions, noise reduction, and energy efficiency [5], [42].

A study by Seyam et al. [43] explored the feasibility of hybrid aircraft propulsion systems that combine traditional turbofans with Molten Carbonate Fuel Cells (MCFCs) to make aviation more sustainable. The researchers analyzed the thermodynamic performance of this hybrid system using five different fuel mixtures: ethanol; methane; hydrogen; dimethyl ether; and methanol. They compared the hybrid system's energy and exergy efficiency, CO₂ emissions, and thrust against a conventional kerosene-powered turbofan. The findings

demonstrated that using alternative fuels and MCFC technology has the potential for greater efficiency and reduced emissions compared to traditional propulsion systems.

While several review papers have discussed the general concepts and modeling approaches for hybrid-electric aviation, there is still a lack of detailed, bottom-up engineering case studies. In this sense, the contribution of this work is not to introduce a methodology, but to present a practical engineering application. By incorporating real experimental data within a bottom-up framework, the study focuses on engineering relevance and offers a mission-level assessment of a realistic retrofit scenario for regional transport aircraft. Moreover, although recent studies have investigated advanced energy management strategies and off-design payload-range optimizations [44], [45], the approach adopted here is simpler, based on a fixed power-split strategy. Even though this simplification does not capture the full complexity of energy management, it makes it easier to clearly understand how battery specific energy influences performance across different mission profiles.

Given the disruptive nature of a hybrid-electric propulsion system in regular aircraft operations, studies and developments in this field are relatively recent, leaving vast room for further research. This work aims to explore the feasibility of using a hybrid-electric propulsion system in a light, multi-engine military transport aircraft. The study is based on the EMB-120 Brasilia, also designated as the C-97 by the Brazilian Air Force. The primary focus is to analyze the system's impact on the aircraft's operational performance, specifically its fuel consumption and climbing capacity. To evaluate the aircraft's performance with both conventional engines and a hybrid-electric system, an in-house software was developed. This software utilizes wind tunnel test data to create an accurate aerodynamic model of the C-97. The in-house software was validated by comparing its results with those from a commercial software program.

II. MATERIALS AND METHODS

The literature on hybrid-electric systems for aircraft indicates that current battery technology makes this alternative unfeasible as a solution for application throughout the entire duration of a long flight. Therefore, this work proposes analyzing, via computer simulation, the feasibility of a hybrid-electric propulsion system for a light transport aircraft. In this system, electric power is applied only during the climb phase, along with fossil fuel, to reduce the number and mass of batteries needed. This allows the gas turbine to be optimized for the cruise phase, where the turboprop is the sole power source,

thereby reducing the mass of kerosene burned. The descent phase is powered in the same way as the cruise phase. For this purpose, two computational models were created: one with a normal turboprop propulsion system and the other a hybrid system, with the intent of making comparisons.

A. Turboprop Engines

To carry out the evaluation of the two propulsive systems, two performance metrics for gas turbines are essential: the Shaft Power Delivered (SPD) and the Power-Specific Fuel Consumption (PSFC). The first indicates how much power the engine can deliver to the propeller shaft [kW], while the second indicates how much fuel is needed for each unit of energy generated on the same shaft [kg/kWh]. These parameters are affected by flight speed and altitude (density, pressure, and temperature), among other factors. To obtain this data, two models were created using available data and the GasTurb® [46] software for calculations: one model for the Pratt & Whitney PW118, and another for the Pratt & Whitney PT6A-68C.

To evaluate the performance of the commuter aircraft chosen for this work, the EMB-120 Brasilia, two different turboprop engines, were studied. The first is the PW118, which is the aircraft's original engine, and the second is the PT6A-68C, which was suggested to be part of a hybrid-electric system primarily due to its lower power-specific fuel consumption and its adequate downsized power output, which suits the hybrid architecture strategy. Both engines are manufactured by Pratt & Whitney. Performance data and certification reports are accessible for both engines, enabling the accurate development of their respective computational models for this comparative analysis.

The EMB-120 Brasilia's propulsion system features two PW118-series turboprop engines [47]. The aircraft's maximum passenger capacity depends on the configuration but can reach 30 people. Additional data is available in Table I.

TABLE I

Basic data obtained from documentation of the EMB-120 Brasilia [47].

Parameter	Value	Unit
Maximum Takeoff Mass (MTOM)	11,990	kg
Operating Empty Mass (OEM)	7,628	kg
Length	20	m
Wing Span	19.78	m

The Pratt & Whitney Canada PW118 is an 1,800 SHP turboprop engine. The data shown in Table II were collected from engine documentation and the European Union Aviation Safety Agency (EASA) Type-Certificate Data Sheet [48]. While some data was not available from the manufacturer, the information that was acquired was fundamental to developing an approximate model using GasTurb®. This turboprop engine equips the EMB-120 Brasilia in both its PW118A and PW118B versions. For this study, the applied data and the developed computational model specifically represent the PW118A version, which serves as the standard baseline powerplant for this aircraft.

The data from Table II was used as target parameters for the design point. This point was defined at Mean Sea Level (MSL) and International Standard Atmosphere (ISA) conditions, with an air speed equal to zero. To achieve this, the configuration was initialized in GasTurb®, a software package that allows for more in-depth performance evaluations by adjusting components' geometry and secondary systems, such as bleeding and cooling [46].

TABLE II

Pratt & Whitney PW118 engine data, taken from the respective documentation and supplemented by reports [48].

Parameter	Value	Unit
Maximum Shaft Power (Mean Sea Level, up to 33°C)	1,342	kW
Maximum Take-Off Torque	10,846	Nm
Maximum Continuous Torque	9,860	Nm
Mass Flow	6.7	kg/s
Pressure Ratio	14:1	
Maximum Take-Off Interturbine Temperature	816	°C
Maximum Continuous Interturbine Temperature	800	°C
Gross Mass	420	kg
Maximum High-Pressure Compressor Bleed	0,25	kg/s

Another factor that should be considered is the maximum temperature at the combustion chamber outlet, which is constrained by metallurgical limits in the absence of advanced cooling technologies. The literature suggests limiting values of 1,200 K (according to Saravanamuttoo et al. [2]) or up to 1,300 K, depending on the alloy [49]. Since this specific data is proprietary information, the temperature values obtained from the engine documentation refer to the Inter-Turbine Temperature (ITT), which is measured between the last stage of the gas generator turbine and the power turbine (PT). Therefore, a value of 1,073.15 K (800 °C) was taken as an upper limit for the PT's entry temperature. The temperature at the

entry of the high-pressure turbine (HPT) was then varied, ensuring it did not exceed 1,300 K. After iterating the parameters to obtain the reference power while observing the established limits, the final values for the model are shown in Table III.

TABLE III
Final parameters values for the Pratt & Whitney PW118 engine model.

Parameter	Value	Unit
Intake Pressure Ratio	99	%
Low-Pressure Compressor Pressure Ratio	3.52	
Low-Pressure Compressor Isentropic Efficiency	85	%
Compressor Inter-duct Pressure Ratio	98	%
High-Pressure Compressor Pressure Ratio	4.06	
High-Pressure Compressor Isentropic Efficiency	84	%
Burner Exit Temperature	1,291	K
Overboard Bleed	0.2	kg/s
High-Pressure Spool Power Offtake	50	kW
High-Pressure Turbine Isentropic Efficiency	88	%
HPT-LPT Inter-duct Pressure Ratio	98.5	%
Low-Pressure Turbine Isentropic Efficiency	88	%
LPT-PT Inter-duct Pressure Ratio	98.5	%
Power Turbine Isentropic Efficiency	87	%
PT Exit Duct Pressure Ratio	97	%
Exhaust-Ambient Pressure Ratio	1.02	%

Using these numerical values, it was possible to achieve the results shown in Table IV at the design point. The SPD value showed only a 0.05 % deviation from the one disclosed in the engine documentation. Regarding temperature limits, the burner exit temperature was set at 1,291 K, and the resultant inter-turbine temperature was 940 K, which is well below the established maximum of 1,073 K.

TABLE IV
Design point results for Pratt & Whitney PW118 engine model.

Parameter	Model Value	Unit
Shaft Power Delivered (SPD)	1,341	kW
Power Specific Fuel Consumption (PSFC)	0.305	kg/kWh

Two types of simulation were performed using the Off-Design mode of GasTurb®. The first was to generate an equilibrium running line to check the model's stability across the working points in the component maps. It is

also noteworthy that, for a better interpretation of the component map, quasi-dimensionless and referred parameters were observed [50], [51]. The resulting running lines confirmed that the model operates within the stability zones of each chart. The second simulation involved assembling a mission profile, including climb, cruise, and descent, to generate SPD and PSFC profiles as a function of the aircraft's altitude and speed. The cruising levels considered were 25,000 ft (FL250) and 26,000 ft (FL260), corresponding to 7,620 m and 7,925 m. A constant climb velocity of 155 kt Calibrated Airspeed (CAS) (79.74 m/s) was determined. The descent was evaluated under a constant air speed of 250 kt CAS, or 128.61 m/s, which corresponds to the aircraft's Maximum Operating Limit Speed (VMO). This high-speed descent strategy is utilized to expedite the flight phase, with the simulation assuming a rapid acceleration at the top of descent. The cruise phase was simulated for both levels, with CAS ranging from 160 kt (82.31 m/s) to 190 kt (97.74 m/s), at intervals of 5 kt. As a result, data were obtained to establish a function to supply the SPD and PSFC values for the model at each flight condition. A short summary of the key propulsion system characteristics is shown in Table V.

TABLE V
PW118 data for gas turbine propulsion model.

Parameter	Model Value	Unit
Number of Prop. Systems	2	
PW118 Mass (each)	420	kg
SPD	Fitted	kW
	Function	
PSFC	Fitted	kg/kWh
	Function	

The Pratt & Whitney PT6A-68C is a 1,600 SHP turboprop engine and a member of the most widely used engine family around the world. Table VI presents data collected from engine documentation and EASA reports [52], which were subsequently used for simulation in GasTurb® [46]. This engine is utilized in this work as the selected gas turbine for the hybrid-electric propulsion system of the EMB-120 Brasilia, primarily due to its available power and reduced fuel consumption (when compared to PW118).

While the PT6A-68C offers lower PSFC, a simple retrofit of the EMB-120 with this engine alone would not be feasible. A gas turbine downsized and optimized for the cruise phase lacks the necessary power output to safely meet the demanding requirements of take-off and climb. Therefore, the hybrid-electric system is essential, utilizing electric motors and batteries to provide the

supplemental power needed during these critical flight phases, enabling the integration of a smaller, more efficient thermal engine.

TABLE VI

Pratt & Whitney PT6A-68C engine data, taken from the respective documentation and supplemented by reports [52].

Parameter	Value	Unit
Maximum Shaft Power (Take-off regime)	1,194	kW
Mass Flow	4.67	kg/s
Pressure Ratio	9.7:1	
Maximum Interturbine Temperature	860	°C
Gross Mass	272	kg
Maximum Gas Generator Bleed	5.25	%

For the development of the PT6A-68C model, the data from Table VI were also considered as target parameters for the design point. This point was defined at MSL and ISA conditions, with an air speed equal to zero. This modeling was also performed using the GasTurb® software. The limit for the ITT is 1,133 K, and the final values for the other parameters are shown in Table VII.

TABLE VII

Final values for parameters of the Pratt & Whitney PT6A-68C.

Parameter	Value	Unit
Intake Pressure Ratio	0.99	
Compressor (HPC) Isentropic Efficiency	86	%
Burner Exit Temperature	1,296	K
Overboard Bleed	0.075	kg/s
High Pressure Spool Power Offtake	20	kW
High Pressure Turbine Isentropic Efficiency	89	%
HPT-PT Inter-duct Pressure Ratio	0.99	
Power Turbine Isentropic Efficiency	89	%
PT Exit Duct Pressure Ratio	0.98	
Exhaust-Ambient Pressure Ratio	1.03	
Nozzle Thrust Coefficient	1	

The results at the design point are shown in Table VIII. The SPD value exhibits a 0.07 % deviation from the figure cited in the engine documentation. The ITT was 1,036 K, which is safely below the established limit.

TABLE VIII

Design point results for Pratt & Whitney PT6A-68C engine model.

Parameter	Model Value	Unit
Shaft Power Delivered (SPD)	1,194	kW
Power Specific Fuel Consumption (PSFC)	0.274	kg/kWh

The same off-design analysis was conducted to obtain data for the SPD and PSFC functions across all flight conditions. The results are shown in Table VIII.

B. Hybrid-Electric Architectures

In this work, three hybrid configurations will be described, highlighting the relevant aspects of each. The first is the series hybrid configuration, in which only the electric motors are connected to the fans or propellers (either directly or through a reduction gearbox). The GT is used solely to drive the generator, which in turn supplies power to the electric motors and the batteries, as illustrated in Fig. 1. This is an adequate system for distributed propulsion, as a single generator can supply several propulsors mounted across the wings and fuselage [53]. These systems benefit from high-aspect-ratio wing structures and high hybridization levels due to the optimal placement of heavy propulsion components [31]. Advantages include the gas turbine being completely decoupled from the thrust or propeller mechanisms, allowing it to operate under optimized conditions. Although this configuration is widely used for road vehicles incorporating piston engines, resulting in lower fuel consumption, it implies a greater weight [9]. Since the electric motor must be sized to supply the entire propulsion power [54], such an architecture is generally considered disadvantageous for aircraft [10].

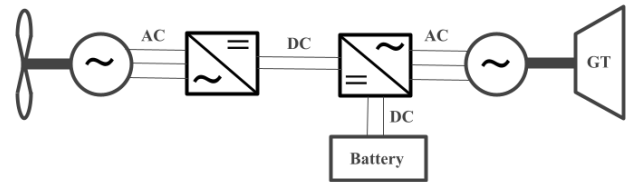


Fig. 1. Series hybrid propulsion schematic (adapted from: Gesell et al. [10]).

The second configuration is parallel hybrid. This system features an electric motor and a GT (the reference engine, [10]) both mounted onto the spool that drives the fan or propeller, allowing both to provide thrust for the aircraft, either independently or together [53]. The gas turbine can also be used to charge the battery pack when the electric machine operates as a generator [54], as shown in Fig. 2. According to Gesell et al. [10], key factors for this design include available space and thermal management, as the components are situated close to one another. To prevent the electric motor from receiving heat from the gas turbine, it is suggested to place the motor in front of the compressor.

This setup allows for better optimization of the GT, as it can operate at higher temperatures and be downsized, resulting in a smaller mass flow. Typically, the electric

power is used for critical phases of flight, such as take-off and climb, and this application largely dictates the battery size [54]. The disadvantages of this concept include the extra mass resulting from the necessary mechanical coupling and gearbox, and a less optimized operating regime for the gas turbine, as it is involved in both electric and propulsive power generation [54].

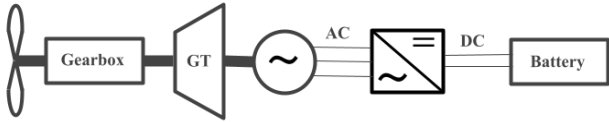


Fig. 2. Parallel hybrid propulsion schematic (adapted from: Gesell et al. [10]).

The third configuration is the series-parallel hybrid. This architecture must have at least one fan or propeller driven by the GT, while at least one other propeller is powered solely by an electric motor (which may also require a reduction gearbox to match the optimal rotational speeds of the motor and the propeller) [53], as shown in Fig. 3. An alternative architecture is often called the power-split system, which consists of a gas turbine, an electric motor, a generator, and a propeller all connected to one another through an epicyclic gear train. This connection allows for flexibility in load distribution, enabling the gas turbine to operate under optimal conditions. A disadvantage of this setup is the complexity added by the planetary gear train, in addition to the increase in overall weight [54].

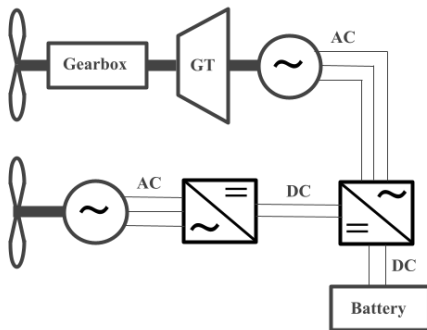


Fig. 3. Series-parallel hybrid propulsion architecture (adapted from: Gesell et al. [10]).

A constant propeller efficiency of 85 % was assumed throughout the mission simulations for both the gas turbine system and the hybrid-electric system. While it is acknowledged that actual propeller efficiency is significantly lower during take-off and low-speed flight phases, this constant value was adopted as a model simplification, reflecting typical cruise and climb performance parameters.

There are various approaches to evaluate the degree of hybridization of a system. Two common methods suggested are to evaluate the split at the energy source or at the entrance of the shaft that drives the propeller [9]. For this research, the power split (S) metric was used:

$$S = \frac{P_{EM}}{P_{shaft}} \quad (1)$$

Where P_{EM} is the shaft power provided by the Electric Motor (EM) only, and P_{shaft} is the total shaft power, coming from the coupled EM and the gas turbine.

The parallel architecture was chosen for the hybrid-electric propulsion system, as shown in Fig. 4. A series architecture is inadequate because it would inherently involve more losses in energy conversion. The series-parallel architecture would also cause a similar penalty, as it would require the inclusion of at least two electric motors in various aircraft locations (such as the wing tips). Furthermore, parallel architecture holds promise in terms of fuel economy and assembly size.

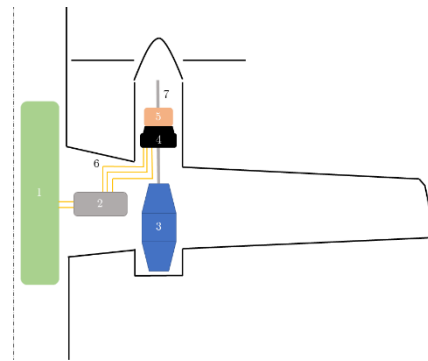


Fig. 4. Schematic of the hybrid-electric system modeled for the EMB-120 Brasilia simulations. 1: Battery-set; 2: Inverter; 3: Turboprop PT6A-68C; 4: Electric motor; 5: Mechanical coupling; 6: Cable-set; 7: Propeller shaft.

Since the electrical components have been modeled using energy conversion efficiency and are assembled in series, the overall efficiency of the electrical system is determined by multiplying the efficiencies of its individual elements. As the electric drive system is mounted in parallel with the turboprop, coupling efficiency must be considered. It is noteworthy that the development of a coupling mechanism that correctly extracts and sums the power from the electric components and the GT is one of the major complications of a parallel system; however, this development is outside the scope of this study. To account for this element, a coupling efficiency of 99 %, which is common for mechanical couplings, was set. It is assumed that the electrical system is directly connected to the propeller shaft, with the overall electrical system efficiency ending at the mechanical power delivered to this coupling.

$$\eta_{electric\ system} = \eta_{batt} \eta_{cab} \eta_{inv} \eta_{EM} \eta_{coup} \quad (2)$$

Where:

$\eta_{electric\ system}$: efficiency of the electric assembly, part of the hybrid-electric system; η_{batt} : efficiency of the battery-set; η_{cab} : efficiency of the cable-set; η_{inv} : efficiency of the inverter; η_{EM} : efficiency of the electric motor; and η_{coup} : efficiency of the mechanical coupling.

It is also worth highlighting that the suggested electric motor and motor drive system require liquid cooling. This cooling system represents a significant component in terms of both mass and efficiency; however, given its complexity, it was not included in this analysis. Therefore, the aircraft will be equipped with two propulsion systems. Each system is composed of a PT6A-68C engine, an electric motor, an inverter, a cable set, and a coupling system. As is common practice in pre-project estimation, a mass is calculated for these primary components, and a 20 % safety margin is added to account for elements and complements that may be integrated later, such as switches, housing, and other auxiliary systems. The baseline masses were derived from commercially available high-performance components: the EMRAX 348 Low Voltage electric motor (41.5 kg) and the Unitek BAMOCAR-PG-D3 inverter (8.5 kg) [55]. The resulting data used for these calculations are shown in Table IX.

TABLE IX
Data for hybrid-electric propulsion model.

Parameter	Value	Unit
Number of Prop. Systems	2	
PT6A-68C Mass (each)	272	kg
SPD	Fitted	kW
PSFC	Function	kg/kWh
	Fitted	
Electric Motor (each)	50	kg
	Energy Consumption	Power
Inverter (each)	Integration	kg
	10	
Cable-Set (each)	24	kg

The efficiencies of the electric system components are displayed in Table X. Common values for state-of-the-art electric components in general are 95 % [3].

TABLE X
Electric system components efficiencies considered.

Parameter	Value	Unit
Electric Motor Efficiency	95	%
Inverter Efficiency	95	%
Cable-Set Efficiency	99	%
Mechanical Coupling Efficiency	99	%
Battery Efficiency	95	%

Batteries are treated separately because, as with fossil fuel, the initial value of their mass is a fundamental output of the simulations. However, to account for internal energy losses, the efficiency in transforming chemical energy into electrical energy was considered constant at 95 % for all tested batteries, which is why it is now included in Table X alongside the other powertrain components. This mass directly alters the aircraft's mass and, consequently, the required lift, in addition to having other consequences.

C. Battery

Most of the high-quality batteries used in mobile applications today rely on Lithium, as it is nature's lightest metal. Early batteries of this type were quite unstable, and the formation of dendrites on the anode during recharging could cause fires. This instability led to the introduction of other elements alongside the metal, resulting in Lithium-ion and Lithium-polymer batteries. The Lithium-polymer subtype requires less casing, which reduces mass and presents high specific energy compared to other types [54].

An important factor to consider is the care that must be taken with the Depth of Discharge. To preserve the quality of the cells, a rule of thumb dictates that a minimum of 3.0 V of voltage or 20 % of the charge capacity must remain at the end of use [23], [54].

Despite their good quality, Lithium-ion batteries are still considerably less capable than fossil fuels in terms of specific energy. Promising future battery chemistries include Lithium-air and other metal-air pairs, such as those based on Aluminum and Iron [15]. Lithium-air batteries, for instance, utilize Lithium at the anode and oxygen taken from the air at the cathode [13], [54]. Consequently, a unique operational challenge of this chemistry is that the battery mass actually increases during flight as atmospheric oxygen is continuously incorporated to form oxides. Another main concern with these advanced battery types is their lower life cycle [13].

D. Electric Components

There are several ways to model electrical components. This can be done in depth, by defining values for voltages, currents, resistances, and losses, and utilizing output parameters such as torque and rotational speeds. Alternatively, if the situation allows, a simplified but still effective approach for preliminary studies is to use efficiency in energy conversion. In this research, modeling by efficiency was chosen and considered adequate for the evaluations carried out. It is important to note that the intent is only to indicate possible components and use them primarily as a reference of mass and power

for the modeled system, not to present them as viable items for joint use.

As with the turboprops, it is important to find a viable solution for electric motorization. Bolam et al. [15] point out two useful measures to analyze this suitability: Specific Power (SP, in kW/kg), which measures power-to-mass performance, allowing for comparison with internal combustion engines; and Torque per unit Rotor Volume (TRV, in kNm/m³), which can be useful when sizing for projects and indicating efficiency in energy conversion. Many existing electric motors for aeronautical applications have an SP ranging between 4 and 10 kW/kg and rotational speeds from 1,300 to 5,000 RPM. Lower speed motors typically have higher torque outputs and, consequently, are better suited for driving large propellers [15]. Brushless direct-current (BLDC) motors and switched reluctance motors are known to be the most suitable for aircraft propulsion due to their high SP and reliability. In addition, new types have been tested, such as axial magnetic field motors with high-temperature superconductors, which can achieve 99 % efficiency [6].

In this work, the 348 EMRAX Low Voltage model was used as a reference for power and mass. This electric motor utilizes a different type of assembly, known as an axial flux synchronous permanent magnet design. It is a three-phase outrunner motor that offers low mass and high torque at low RPM, featuring a mixed cooling system (air and liquid) [56]. Table XI presents additional data obtained from manufacturer publications [56].

TABLE XI

Manual data for the 348 EMRAX low voltage motor [56].

Parameter	Value	Unit
Efficiency	92– 98	%
Outer Diameter	348	mm
Axial Length	107	mm
Maximum Battery Voltage	420 (at 4,000 rpm)	VDC
Maximum Motor Current	1,100	A_{rms}
Continuous Motor Current	550	A_{rms}
Peak Motor Power at Max RPM	380	kW
Continuous Motor Power at Load RPM	210	kW
Maximum Motor Torque	1,000	Nm
Continuous Motor Torque	500	Nm
Maximum Rotational Speed	4,000	rpm
Mass	41.5	kg

E. Fuel and Battery Power Consumption

• Fuel consumption

In a longitudinal steady flight lift equals mass, but fuel is consumed throughout the mission, causing the aircraft's

mass to decrease [57]. Therefore, the necessary lift to sustain flight, changes. The way to account for it is shown below:

$$\frac{dm}{dt} = cP_{shaft,GT} \quad (3)$$

Where:

dm/dt : aircraft mass variation in time due to fuel consumption [kg/s].

c : PSFC of the gas turbine, evaluated at the given flight condition using the previously established polynomial fitting functions. These functions correlate the PSFC with the aircraft's altitude (during climb and descent phases) or air speed (during the cruise phase) [kg/kWh] (with appropriate unit conversions applied during integration).

This formulation will be used for both the gas turbine models: PW118 and PT6A68C.

• Battery Energy Consumption

Unlike the fuel situation, the decrease in battery charge causes negligible mass variation for traditional closed-cell batteries. While it is acknowledged that specific advanced chemistries, such as Lithium-air, experience a mass increase during discharge, the overall battery mass is considered constant throughout the mission as a model simplification. Therefore, its energy consumption (in kWh) will be calculated directly from the demanded power of the electric system and the working time in the hybrid-electric propulsion simulation.

One of the established requirements is that the batteries conclude their period of use—specifically, the climb phase—with approximately 20 % of remaining charge. This residual charge value is intended to preserve the charging and discharging capacity, as well as to extend the batteries' lifetime.

With the perspective of testing both generic battery models currently available on the market and those projected for future developments, six multiples of 125 Wh/kg were applied as pack-level battery specific energy. It is important to note that these figures represent pack-level values. Unlike cell-level specific energy cited in the broader literature, pack-level values account for the added mass of the BMS, thermal management, and structural enclosures, making them significantly lower but more realistic for aircraft integration. Thus, batteries ranging from 250 Wh/kg, representing the state-of-the-art of current off-the-shelf technology, up to 750 Wh/kg were simulated. The 750 Wh/kg pack-level specific energy should be interpreted as an extreme upper bound associated with far-future technological developments, rather than a guaranteed baseline for 2035.

It is important to emphasize that the specific energy values considered here refer to the Battery Energy Density (BED) at the pack level, rather than at the cell level. In practical aircraft applications, integration requires additional mass for cooling systems, structural casing, and safety containment, which substantially reduces the effective specific energy. Based on recent analyses in the literature [18], [58], pack-level BED values in the range of 250–300 Wh/kg can be regarded as realistic assumptions in the near term. In contrast, values as high as 750 Wh/kg should be interpreted as future scenarios. They are not intended to suggest near-term feasibility, but rather to define an upper bound and to help identify the technological thresholds at which hybrid-electric propulsion may begin to deliver meaningful mission-level benefits. The efficiency in transforming chemical energy into electrical energy was considered constant and set at 95 % for all tested batteries. Furthermore, they are not recharged in flight, meaning they are placed in the aircraft fully charged for the mission.

Another factor that affects the required battery mass is power splitting. To facilitate comparisons, missions were simulated using six different power split values, ranging from 5 % to 30 % (in 5 % intervals). While high hybridization levels (such as 30 %) exceed the individual capacity of the reference EMRAX motor—requiring a multi-motor association in a real-world application, as will be discussed in the results section—this spectrum covers several splits referenced in the literature, such as those discussed by Gesell et al. [10] and Voskuijl et al. [9], and was tested against each value of battery specific energy.

F. Aircraft Performance Analysis

The main stage of the study was to evaluate the performance of the EMB-120 Brasilia aircraft using two different types of propulsion systems. In this study, we were able to access the wind tunnel test reports for the EMB-120 Brasilia, which provided practical values for the dimensionless lift and drag coefficients (C_L and C_D). Given the sensitive nature of this documentation, the data will be shown normalized below.

- **Experimental Dimensionless Lift Coefficient**

Figure 5 shows the normalized data for the Lift Coefficient (C_L) as a function of the Angle of Attack (α or AoA), excluding values beyond the maximum point of the curve. An almost linear slope is visible up to approximately 30 % of the maximum AoA. Since most normal flight operations (climb, cruise, and descent) occur in low AoA regions, the theoretical linear approximation

is valid for most of the analyses. A fitted function was subsequently implemented to supply the model with α data.

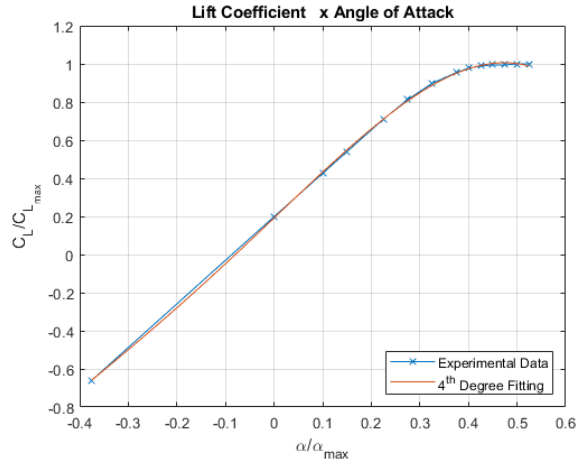


Fig. 5. Normalized experimental data for C_L vs. α along with fitting function curve obtained with Matlab®.

- **Experimental Dimensionless Drag Coefficient**

The same process was repeated for the drag coefficient values, although it was not necessary to discard any point for a better fit, the results are shown in Fig. 6.

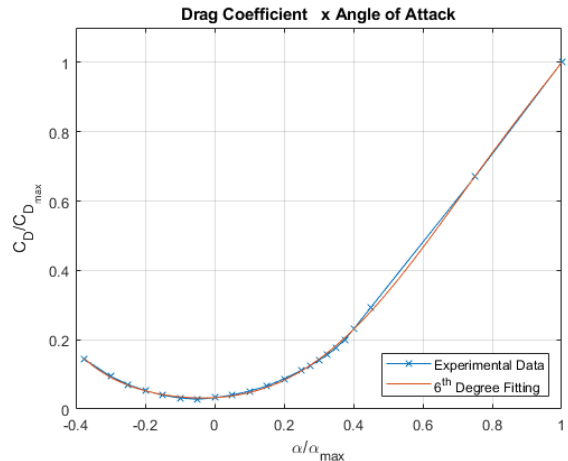


Fig. 6. Normalized experimental data for C_D vs. α along with fitting function curve obtained with Matlab®.

G. Flight Performance Simulation

Complete flight simulations of the EMB-120 Brasilia were conducted to evaluate its performance, comparing the traditional turboprop engine to a hybrid-electric propulsion system. The study's objective was to determine the feasibility of adopting a hybrid-electric system for short-range commuter missions, focusing on the exclusive use of electrical energy during the critical climb phase.

The EMB-120 Brasilia is extensively used by the Brazilian Air Force for various missions. A common flight plan for this aircraft is the route from Brasília (DF), the capital of Brazil, to Rio de Janeiro (RJ). These cities are separated by approximately 500 NM (926 km), which is considered a suitable short-range mission for these simulations. For simplification, both the departure and arrival airports were assumed to be located at MSL. The analysis focused exclusively on the longer flight segments—climb, cruise, and descent—as these account for the greatest energy demand. Take-off and landing were excluded from the study's scope. The take-off phase, which demands the greatest power, involves non-steady flight, as the aircraft accelerates to rotation and then climb speeds. Similarly, the landing phase, which also requires differential analysis due to deceleration and has a minor impact on fuel consumption, was also omitted. Consequently, the climb phase is defined as beginning at MSL, the same altitude where the descent phase concludes.

In compliance with flight regulations and standard operating procedures (SOPs), the cruise altitude was fixed at 25,000 ft (FL250), or 7,620 m. Brazilian flight regulations also mandate that an aircraft on a navigation mission must carry reserves, specifically fuel to reach its destination, divert to an alternative airport, and hold for 45 minutes. For simplification, these required reserves were converted into a final mandatory residual fuel of 500 kg. The initial fuel load needed will be a key output of the simulations. This figure directly reflects the total mission fuel burn, thus justifying or disproving the hybrid-electric architecture's viability as a fuel and emissions saver.

Airspeed is a critical planning factor. The airspeed employed in the lift and drag equations is the CAS. However, the True Airspeed (TAS) must be used for computing the distance traveled over the ground, consistent with the static atmosphere concept. Furthermore, for speeds exceeding Mach 0.30, air compressibility effects become significant [59], necessitating corresponding corrections. The implemented conversion procedure is robust, validating the model for both compressible and incompressible subsonic flows [60].

The simulation employs a specific methodology for the climb ratio (V_{climb}) to closely reflect real-world operating conditions. The model is initially configured to climb at 1,500 ft/min until the available power from the propulsion system can no longer sustain these flight conditions. At this point, the vertical speed is progressively reduced so that the required power matches the available power. For the descent rate ($V_{descent}$), the model maintains a rate of -1,500ft/min until reaching 2,000ft Above Ground Level

(AGL). Thereafter, the descent rate is reduced to -1,000ft/min for the remainder of the phase.

The OEM is established at 8,000 kg, with a MTOM of 11,990 kg. When considering the new propulsion system, the gross mass of the aircraft's original engine, the PW118 (420 kg), is subtracted from OEM. This 420 kg is added back when simulating the turboprop-only system. Alternatively, for the hybrid-electric configuration, the PW118 is replaced by the combined mass of the PT6A-68C engine (272 kg) and the electrical components (electric motor, inverter, and cable-set). This leaves 4,410 kg available for the distribution of the propulsion systems, fuel, batteries, and payload. As the aircraft's objective is to transport passengers or general cargo, a constant payload of 1,000 kg was set for all simulations. It must be remarked that this value is lower than the standard 30-passenger capacity of the conventional EMB-120 (which corresponds to approximately 3,000 kg). This payload reduction was adopted as a necessary trade-off to accommodate the heavy battery packs and electrical components while respecting the aircraft's MTOM limits. A summary of these parameters is presented in Table XII.

Remember that:

$$ABM = \text{Aircraft Mass Without Engine} + \text{Propulsion System's Mass} \quad (4)$$

TABLE XII
Proposed parameters for the simulated missions with EMB-120 Brasilia.

Parameter	Value	Unit
Mission Range	926	km
Departure Airdrome Altitude	0	m
Cruise Altitude	7,620	m
Arrival Airdrome Altitude	0	m
Aircraft Mass Without Engines	7,160	kg
Aircraft Maximum Take-Off Mass	11,990	kg
Mandatory Residual Fuel When Landing	500	kg
Payload	1,000	kg
CAS Climb Phase	79.74	m/s
Initial Climb Rate	7.62	m/s
CAS Cruise Phase	87.19	m/s
CAS Descent Phase	128.61	m/s
Initial Descent Rate	-7.62	m/s

H. Simulation Algorithms

All algorithms were developed and implemented using the Matlab® software. While steady flight performance analysis relies on the balance of forces acting on the aircraft, simulating a complete mission involves dynamic variations in flight conditions. These variations include

changes in mass (due to fuel consumption), air density (due to altitude changes), and fluctuations in available power, among other factors.

To accommodate such variations, their effects were integrated dynamically throughout the simulations. Since the codes were developed in Matlab®, the *ode45* solver was employed for this task. The *ode45* integrator is specifically designed for solving no stiff differential equations using a Runge-Kutta method with a variable time step. By utilizing this method, it was possible to track the variations and consequences related to the aircraft's mass, AoA, altitude, and ground distance covered.

I. Algorithm for Hybrid-Electric Powered Mission

The main routine of the hybrid-electric simulation algorithm must iteratively account for the battery mass. Therefore, it incorporates an additional loop within the climb sector of the code. The main inputs for this routine are the same as those for the turboprop-only case, with the inclusion of two key parameters: the battery type (defined by its specific energy) and the power split for the climb phase of the mission.

To ensure the reliability of the quantitative comparisons presented, it is important to define the limits of the integrated framework. From a methodological perspective, the aerodynamic and conventional propulsion models can be considered fully validated: the aircraft model is based on for the EMB-120, and the gas turbine performance is validated using GasTurb®. In contrast, the electrical powertrain components are only partially verified, which electric motors, inverters, and batteries are represented through macroscopic specific-mass and efficiency parameters, rather than high-fidelity transient models. As a result, complex aspects, such as dynamic thermal management, are treated in a simplified manner. Therefore, while the framework is well suited for preliminary sizing and mission-level fuel consumption estimates, it is not intended for detailed subsystem-level analyses or transient stability assessments.

III. RESULTS AND DISCUSSION

A. Turboprop System Simulation Results

A summary of the most significant data for this study, concerning the simulation of the aircraft in its original, turboprop-only configuration, is presented in Table XIII. Initially, two key convergence criteria of the algorithm are highlighted: the successful completion of the 926 km route with accuracy, and the maintenance of the mandatory final fuel reserve of 500 kg in the tanks.

The fourth column presents the fuel consumed along the flight path, a crucial factor for the subsequent comparison with the hybrid-electric case. The next parameter corresponds to the aircraft's Take-Off Mass (TOM) for the mission, which must remain below the established MTOM of 11,990 kg. Finally, the table includes the time taken to climb to cruise altitude and the total flight time, both of which serve as key metrics for comparison with the hybrid configuration.

TABLE XIII
Simulation results for the turboprop system case.

Prop. System	Distance Flown [km]	Final Fuel [kg]	Burned Fuel [kg]	Take-Off Mass [kg]	Climb Time [min]
Turboprop	926	500	1,089	10,589	23.4

B. Hybrid-Electric System Simulations

The results for the hybrid-electric cases are presented in Table XIV. The first row features the results for the turboprop-only case to provide a direct basis for comparison. This table details the fuel consumption, relevant masses, and climb times calculated from the simulations.

Regarding the iteration criteria for the simulations, all 37 cases successfully converged to the exact 926 km flight distance. Likewise, all cases showed adequate convergence to the final fuel target of 500 kg and the 20 % final battery charge, with only negligible deviations (maximum fuel deviation of 0.80 kg, which constitutes only 0.02 % of the target value). The case involving the lower performance batteries, specifically those with 125 Wh/kg, requires careful evaluation. For a 5 % power split, good convergence was achieved. However, for power splits ranging from 10 % to 30 %, the simulation criteria were not met. This failure, resulting from either not reaching the cruising altitude at the specified time or exceeding the MTOM, indicates that these configurations are not feasible flight options. Consequently, the only valid configuration for the 125 Wh/kg batteries is the 5 % power split. For all other battery specific energy levels, every simulated case yielded valid results.

A general analysis of Table XIV indicates that the climb time is reduced as both the battery specific energy and the power split increase. This outcome can be attributed to the assumption that electric motors maintain practically constant energy conversion efficiency regardless of altitude and the resulting ISA variations. Therefore, if a portion of the shaft power is supplied by the electrical system, and this percentage is increased, the total available shaft power increases, and the aircraft

becomes more capable of sustaining steeper climbing conditions and maintaining a high rate of climb for a longer duration. However, exceptions were noted: the 5 % power split cases for the 125 Wh/kg, 250 Wh/kg, and 375 Wh/kg batteries resulted in longer climb times than the purely gas turbine configuration. In these instances, the greater availability of power was insufficient to overcome the significant mass penalty imposed by these lower specific energy batteries.

Regarding the total flight time, it was observed that batteries with higher specific energies generally lead to a very slight decrease in total flight time. This must be understood in the context that electrical energy is used only during the climb phase. For the remainder of the flight, the aircraft must carry the mass penalty of the batteries and electrical components, despite the reduction in the required fuel amount. Since the ascent phase is significantly shorter compared to the cruise and descent phases, even a considerable reduction in its duration such as the 20.9 % decrease observed for the case with E_{batt} of

500 Wh/kg and an S of 25 % results in a proportionally much smaller reduction in the total flight time, specifically 0.5 %.

Analysis of Table XIV confirms that, for the valid cases, fossil fuel savings achieved through hybridization increase as the power split value decreases. This relationship is established because smaller power splits require lower battery masses, which subsequently results in a reduced power demand on the gas turbine during the remaining flight phases. It must be noted, however, that the difference in fuel savings between 5 % and 30 % power split diminishes significantly as the battery specific energy improves. This variation is demonstrated by the following examples:

- For batteries with 0.250 kWh/kg: savings range from 17.80 % (5 % S) down to 6.88 % (30 % S).
- For batteries with 0.750 kWh/kg: savings range from 19.29 % (5 % S) down to 16.96 % (30% S).

TABLE XIV

Simulation results of burned fuel, battery mass, take-off mass, and climb time for the hybrid-electric cases. The deviations are shown in relation to the values of the conventional turboprop system simulation.

E_{batt} [Wh/kg]	S [%]	Burned Fuel [kg]	Deviation [%]	Battery Mass [kg]	Take-Off Mass [kg]	Climb Time [min]	Deviation [%]
Turboprop Syst.		1,089	-	-	10,589	23.7	-
125	5	926	-15.01	340	10,638	26.6	12.15
	5	895	-17.80	156	10,423	24.3	2.41
	10	918	-15.74	313	10,603	23.4	-1.40
	15	940	-13.64	469	10,781	22.4	-5.64
	20	964	-11.48	624	10,960	21.5	-9.64
	25	989	-9.20	781	11,141	20.6	-13.22
250	30	1014	-6.88	935	11,321	19.7	-16.90
	5	887	-18.56	102	10,361	23.8	0.44
	10	899	-17.40	200	10,471	22.4	-5.56
	15	912	-16.22	295	10,579	21.2	-10.53
	20	925	-15.06	387	10,684	20.2	-15.08
	25	938	-13.89	477	10,787	19.2	-19.04
375	30	951	-12.69	567	10,890	18.4	-22.37
	5	883	-18.93	76	10,331	23.6	-0.48
	10	892	-18.12	148	10,411	22.1	-6.85
	15	900	-17.33	216	10,489	20.8	-12.33
	20	909	-16.55	282	10,563	19.7	-16.93
	25	917	-15.76	347	10,636	18.8	-20.91
500	30	926	-14.95	411	10,709	18.0	-23.87
	5	880	-19.15	60	10,313	23.4	-1.28
	10	887	-18.54	117	10,376	21.9	-7.71
	15	893	-17.95	171	10,436	20.6	-13.24
	20	900	-17.38	222	10,494	19.5	-17.90
	25	906	-16.80	273	10,551	18.6	-21.82
625	30	913	-16.19	323	10,608	17.9	-24.63
	5	879	-19.29	50	10,301	23.4	-1.54
	10	884	-18.83	97	10,353	21.7	-8.48
	15	889	-18.36	141	10,402	20.4	-13.94
	20	894	-17.91	184	10,450	19.4	-18.44
	25	899	-17.46	225	10,496	18.4	-22.51
750	30	904	-16.96	266	10,543	17.8	-25.08

Figure 7 displays the altitude curves as a function of time for all tested hybrid configurations. It is important to highlight, particularly in the graph for batteries with a specific energy of 125 Wh/kg, that only the configuration with a 5 % power split successfully reached the cruise altitude. All other configurations for this battery type failed to reach the target altitude and instead completed the cruise phase while maintaining the altitude they had achieved when the designated climb time expired, consistent with the constraints previously discussed. Regarding the other battery types, a clear trend is evident: for a given battery specific energy, an increase in the power split results in the cruising altitude being reached faster, despite the associated penalty of a heavier battery set.

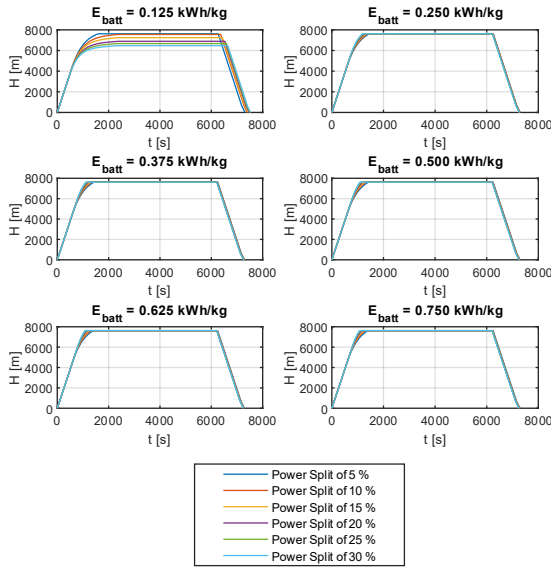


Fig. 7. Altitude vs time curves for all battery-specific energy and power split situations simulated.

C. Comparison of Highlighted Simulation Results

To highlight important characteristics and facilitate the observation of specific trends, this section presents comparisons between the results obtained for 250 Wh/kg batteries - considered the current state-of-the-art - and those for 750 Wh/kg batteries, which are expected to be available in the far future. The initial discussion focuses on the variation of battery masses in relation to their specific energy (E_{batt}) and the applied power split. While all results are tabulated in Table XIV, Figure 8 provides a clear graphical representation of these relationships.

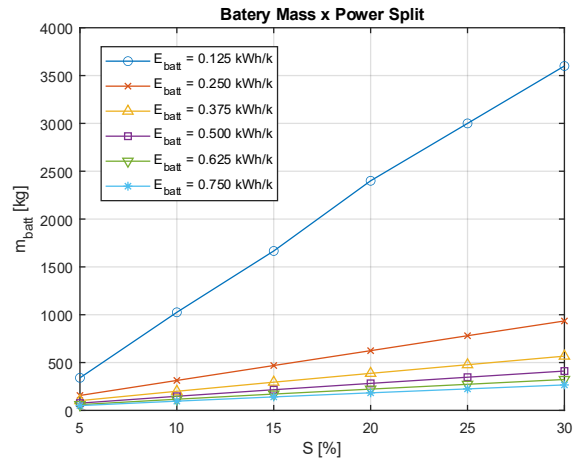


Fig. 8. Simulation results for battery masses in hybrid cases.

The simulation iterative criteria were not met by the 125 Wh/kg battery specific energy curve, except for the 5% power split case. Comparing the 250 Wh/kg and 750 Wh/kg battery curves, a substantial decrease in battery mass was observed. These decreases ranged from 67.97 % (5 % S) to 71.51 % (30 % S) when referring to the 250 Wh/kg battery type, as detailed in Table XV. It is also noted that the percentage mass reduction for each case increases with power split. Conversely, and as expected, the absolute battery mass increases as the power split progresses.

The following paragraphs present the simulation results for the conventional turboprop engine alongside four selected hybrid-electric cases for comparison. This selection was strategically made using the 250 Wh/kg and 750 Wh/kg batteries, coupled with the 5 % and 30 % power splits. These four configurations were chosen because the 5 % power split maximizes fuel economy, while the 30 % power split provides the greatest reduction in climb time, as demonstrated in Table XVI.

TABLE XV

Comparison between simulation results for battery masses in hybrid cases with batteries of 250 and 750 Wh/kg of specific energy. The percentage deviations are taken in reference to the first battery type.

S [%]	Battery Mass for $E_{batt}=250$ Wh/kg [kg]	Battery Mass for $E_{batt}=750$ Wh/kg [kg]	Deviation [%]
5	156	49	-68.0
10	313	96	-69.1
15	469	141	-67.0
20	624	183	-71.0
25	780	224	-71.2
30	934	266	-71.5

TABLE XVI

Summary of simulations results for selected cases (battery specific energy of 250 and 750 Wh/kg). The deviations are shown in relation to the values of the conventional turboprop system simulation.

E_{batt} [Wh/kg]	S [%]	Burned Fuel [kg]	Deviation [%]	Climb Time [min]	Deviation [%]
Turboprop Syst.		1,089	-	23.7	-
250	5	895	-17.8	24.3	2.4
	30	1,014	-6.9	19.7	-16.9
750	5	879	-19.3	23.4	-1.5
	30	904	-16.9	17.8	-25.0

Figure 9, which illustrates the TOMs and the subsequent variation of the aircraft's mass during flight, shows that the curves for the hybrid-electric cases are practically parallel. This parallelism exists because the mass variation throughout the mission is primarily driven by fuel consumption, and all hybrid configurations utilize the same gas turbine engine (PT6A-68C). However, minor differences in slope are expected between the hybrid curves. This is because varying specific energies and power splits result in different battery masses, which in turn lead to distinct lift and drag coefficients being applied throughout the flight. The mass variation curve for the aircraft with the conventional turboprop engine (PW118) crosses the hybrid curves. This is due to its differing fuel consumption rate resulting from the use of a distinct engine model. Furthermore, the discrepancy in the TOM of the 30 % power split configuration with current batteries (250 Wh/kg) is noteworthy. Specific values for all TOMs can be found in Table XIV.

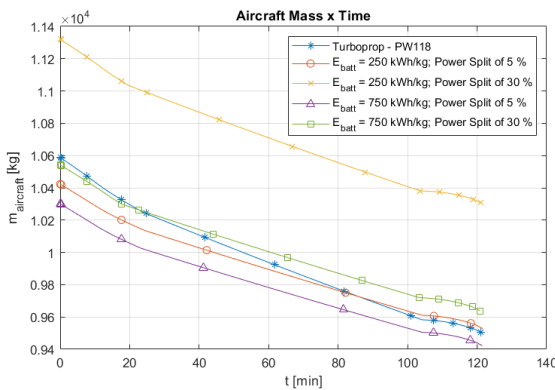


Fig. 9. Aircraft total mass vs time results for selected cases: turboprop PW118 system and hybrid-electric systems with battery specific energies of 250 and 750 Wh/kg, and power splits of 5 % and 30 %.

Observing Fig. 10, which illustrates the power required to maintain flight under the given conditions, the superior

ability of configurations with larger power splits to sustain a climb rate of 1,500 ft/min for a longer duration is again evident, resulting in them reaching cruise altitude first.

For current batteries (250 Wh/kg), the highest climb rate was maintained up to 17,445 ft, while for future batteries (750 Wh/kg), it reached 18,953 ft. For the lower power splits (5 % S), this maximum altitude was close to 14,453 ft for both battery types. The key difference between these lower-split cases lies only in the subsequent rate of climb maintained, as will be shown later in Fig. 13.

Compared to the gas turbine-only system, the 5 % power split configuration with 250 Wh/kg batteries resulted in a slightly longer climb time, whereas the same split with 750 Wh/kg batteries yielded a slightly shorter one.

It is also notable that although the 30 % power split configurations reach cruise altitude faster, their optimal descent points were very similar to the others, which explains the minor changes observed in the total flight time. The power curve required for the 30 % split with current batteries was higher during the cruise phase due to the greater Total Aircraft Mass (TAM). This specific configuration began the cruise phase with a mass of 11,034 kg, significantly higher than the 10,250 kg value for the turboprop-only system.

The climb phase exhibits an initial increase in power required, followed by a subsequent decrease until the end of the phase. This initial growth is dictated by the model's strategy to maintain the initial climb rate of 1,500 ft/min. Maintaining this constant vertical speed demands progressively more power due to the combination of increasing altitude and decreasing air density, a trend that continues until the available propulsion power is no longer sufficient for this flight condition.

For the descent phase, the power required increases as the aircraft's altitude decreases due to the corresponding growth in air density. At 7,176.20 s (119.60 min), an anomalous leap in demanded power is observed in the curve. This is because the aircraft have reached the 2,000 ft threshold AGL, triggering the programmed reduction of the descent rate from 1,500 ft/min to 1,000 ft/min (5.08 m/s).

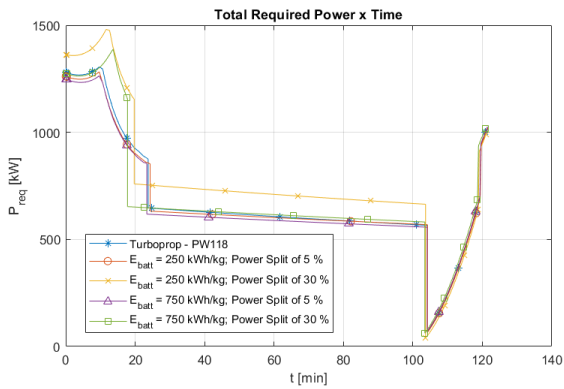


Fig. 10. Required shaft power per propeller vs time results for selected cases: turboprop PW118 system and hybrid-electric systems with battery specific energies of 0.250 and 0.750 kWh/kg, and power splits of 5 % and 30 %.

Figure 11 illustrates that the power demanded from the fossil fuel engine was highest for the conventional PW118 motorization. As anticipated, the power demand on the gas turbine engine (PT6A-68C) decreased as the power split increased. The cruise power required by the configuration with 250 Wh/kg batteries and a 30 % power split was noticeably higher than the others, a difference directly attributable to the higher initial aircraft mass for that phase. Furthermore, the power curve originating from the PW118 engine began the cruise phase at levels like the 30 % power split hybrid configuration with 750 Wh/kg batteries but finished at levels corresponding to the 5 % power split with 250 Wh/kg batteries. This demonstrates the distinct fuel consumption pattern and efficiency of the conventional PW118 engine relative to the hybrid configurations.

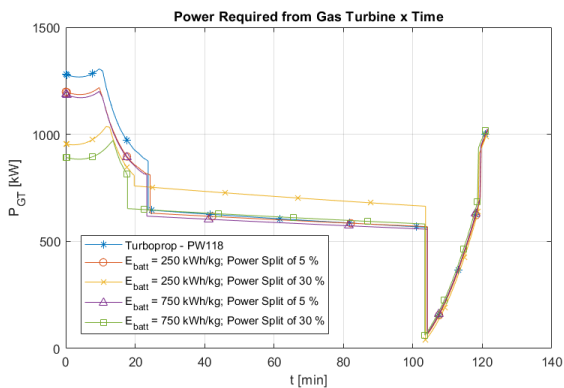


Fig. 11. Turboprop shaft power required per propeller vs time results for selected cases: turboprop PW118 system and hybrid-electric systems with battery specific energies of 0.250 and 0.750 kWh/kg, and power splits of 5 % and 30 %.

Figure 12 illustrates the demand for electrical power. For configurations utilizing the 5 % power split, the power values required were practically indistinguishable, though the demand duration was slightly longer for the current (250 Wh/kg) batteries. It is noteworthy that the electric motor chosen for the model is sufficient to meet the power requirements of both these 5 % S configurations. However, for the 30% power splits, the power demanded by the 250 Wh/kg batteries was significantly greater than that required by the 750 Wh/kg batteries, a difference attributable to the substantial added mass penalty. In this specific high-demand case, an association (or parallel arrangement) of the adopted electric motors, or the selection of an alternative EM, must be established to successfully meet the required power demand. It is important to clarify that the additional mass penalty of such a multi-motor arrangement (estimated at approximately 120 kg for duplicating the motors and inverters on both sides) was not accounted for in the current simulations.

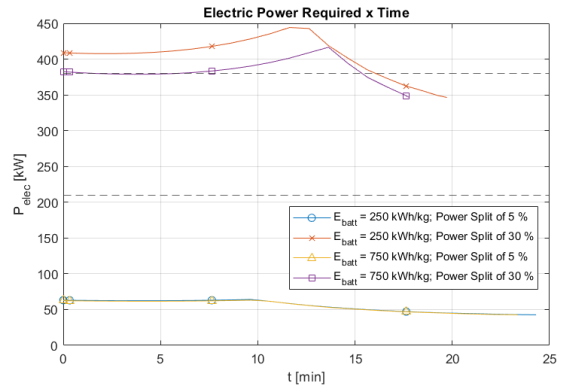


Fig. 12. Electric shaft power required per propeller vs time results for selected cases: turboprop system and hybrid-electric systems with battery specific energies of 0.250 and 0.750 kWh/kg, and power splits of 5 % and 30 %.

Figure 13 displays the climb rates maintained as a function of altitude. It is again evident that configurations utilizing a 30 % power split sustained the initial climb rate of 1,500 ft/min up to significantly higher altitudes. This is primarily justified by the electric motors' constant efficiency regardless of altitude, a key advantage over gas turbines, which experience a predictable loss of available power as altitude increases. The 5 % power split configurations demonstrated a capability for the maximum climb rate as a function of altitude that was comparable to the pure turboprop engine (PW118). For current batteries (250 Wh/kg), the climb rate maintained after the point of maximum performance was consistently lower than that of the PW118 engine. For future batteries (750 Wh/kg), however, the hybrid system's climb rate

surpassed the conventional engine's curve at approximately 20,379 ft. This crossover occurs because the gas turbine's available power continues to decrease with increasing altitude, while the hybrid system maintains a more favorable power profile.

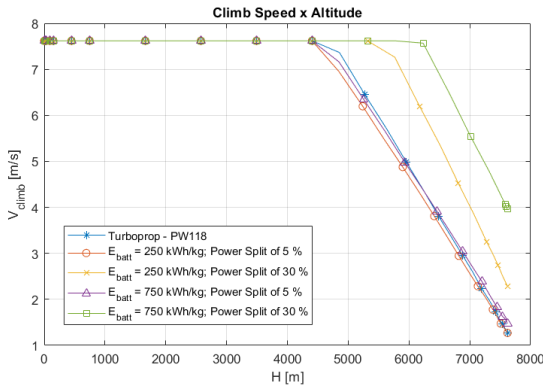


Fig. 13. Climb rate vs altitude results for selected cases: turboprop PW118 system and hybrid-electric systems with battery specific energies of 0.250 and 0.750 kWh/kg, and power splits of 5% and 30%.

To better visualize the fundamental trade-off between fuel consumption and climb performance, a Pareto-type graph is presented in Fig. 14. This figure plots the climb time against the total mission fuel burn for each valid battery specific energy case across the tested power splits. The performance of the reference conventional turboprop aircraft is also included as a baseline. It is visible how different hybridization strategies push the performance towards either greater fuel savings (lower power splits) or faster climb times (higher power splits), and how future battery technologies (higher specific energies) shift the entire Pareto front toward a more optimal combined performance.

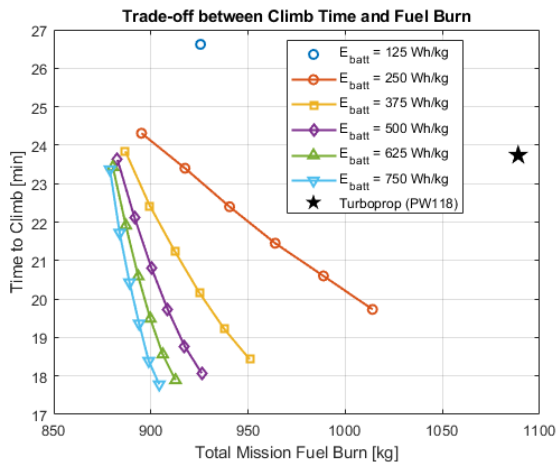


Fig. 14. Pareto-type graph illustrates the trade-off between climb time and total mission fuel burn for the simulated

hybrid-electric cases across different battery specific energies and power splits, compared to the baseline turboprop aircraft.

IV. CONCLUSION

This study evaluated different hybrid-electric propulsion system architectures for commuter aircraft. The parallel configuration was identified as the most viable due to its potential for fuel savings, achieved by optimizing the gas turbine, and the minimal modifications required for the proposed retrofit. To assess the performance of a commuter aircraft with a hybrid-electric system, mathematical models were developed for the PW118 and PT6A-68C gas turbines.

These models, created using commercial software, are considered verified within the limitations of available engine data. The aircraft performance model was based on experimental wind tunnel data for the EMB-120 Brasilia's lift and drag coefficients. While simplifications were made in the hybrid models for the electrical components, safety factors, such as a 20 % mass increase per element, were included. The study yielded consistent results, allowing for a direct comparison between the performance of the traditional and hybrid-electric configurations. Batteries were simulated based on their generalized energy density, encompassing both current and future technologies. The 250 Wh/kg value was used for current state-of-the-art batteries, while 750 Wh/kg represented an extreme upper bound associated with far-future scenarios.

Power split configurations greater than 10 % proved unfeasible for the 125 Wh/kg batteries. It was specifically compared two power splits, 5 % and 30 %, for the two highlighted battery types. The 5 % power split was more effective for fuel economy, reducing kerosene burn by up to 19.3 % with the 750 Wh/kg batteries. Even with current 250 Wh/kg batteries, a notable fuel saving of up to 17.8 % was possible. Conversely, the 30 % power split delivered greater reductions in climb time. With 250 Wh/kg batteries, climb time was reduced by 16.9 %, and with 750 Wh/kg batteries, it was reduced by an impressive 25.1 %. Interestingly, the difference in fuel economy between the two power splits decreased as battery quality improved, suggesting that mass remains a critical factor. For the best current batteries (250 Wh/kg), the 5 % and 30 % power splits saved 17.8 % and 6.9 % of fuel, respectively. For the projected 2035 batteries, these numbers were 19.3% and 16.9 %. This shows that with current technology; a trade-off exists between saving fuel and reducing climb time. However, as battery technology evolves, it may be possible to achieve both outcomes simultaneously.

Finally, it must be acknowledged that the substantial mass penalty imposed by current and near-future battery

technologies necessitates a significant reduction in payload capacity. Consequently, the operational business case for such a hybrid-electric retrofit differs from the standard high-density commuter role of the conventional EMB-120, shifting its potential applicability towards lower-density regional transport, executive aviation, or specific cargo missions where lower fuel consumption and reduced emissions are prioritized over maximum passenger capacity.

ACKNOWLEDGMENT

The authors would like to thank ITA (Aeronautics Institute of Technology), Department of Turbomachines, for the support and infrastructure provided during this research work; as well as the Coordenação de Aperfeiçoamento de Pessoal de Nível Superior - Brazil (CAPES - Higher Education Improvement Coordination); Conselho Nacional de Desenvolvimento Científico e Tecnológico (CNPq - Brazilian National Council for Scientific and Technological Development, Brazil); FINEP (Financiadora de Estudos e Projetos) pelo projeto Captaer III, número do projeto 01.22.0313.00; FLYMOV - Engineering Research Center, grant number 2021/11258-5, Sao Paulo Research Foundation (FAPESP).

The Article Processing Charge for the publication of this research was funded by the Coordenação de Aperfeiçoamento de Pessoal de Nível Superior (CAPES), Brazil (ROR identifier: 00x0ma614). For open access purposes, the authors have assigned the Creative Commons CC BY license to any accepted version of the article.

The authors declare no competing financial interest.

REFERENCES

- [1] ATAG. Air Transport Action Group, "Facts & figures," 2020. <https://www.atag.org/facts-figures> (accessed Jun. 15, 2021).
- [2] G. F. C. R. H.I.H. Saravanamuttoo, H. Cohen and P. V. S. A.C. Nix, *Gas Turbine Theory*, 7th ed. United Kingdom: Pearson Education Limited, 2017.
- [3] A. H. Epstein and S. M. O'Flarity, "Considerations for reducing aviation's CO₂ with aircraft electric propulsion," *J. Propuls. Power*, vol. 35, no. 3, pp. 572–582, 2019, doi: 10.2514/1.B37015.
- [4] M. Marwa, S. M. Martin, B. C. Martos, and R. P. Anderson, "Analytic and numeric forms for the performance of propeller-powered electric and hybrid aircraft," 2017. doi: 10.2514/6.2017-0211.
- [5] S. Sahoo, X. Zhao, and K. Kyprianidis, "A review of concepts, benefits, and challenges for future electrical propulsion-based aircraft," *Aerospace*, vol. 7, no. 4, 2020, doi: 10.3390/aerospace7040044.
- [6] A. Kozakiewicz and T. Grzegorzczak, "Electric Aircraft Propulsion," *J. KONBiN*, vol. 51, no. 4, pp. 49–66, Dec. 2021, doi: 10.2478/JOK-2021-0044.
- [7] G. N. Barufaldi, M. A. V. Morales, and R. G. A. da Silva, "Parametric determination of fuel consumption during cruise flight for fuel cell powered airplanes," *J. Brazilian Soc. Mech. Sci. Eng.*, vol. 44, no. 3, pp. 1–10, 2022, doi: 10.1007/s40430-022-03383-4.
- [8] B. Wang, Q. Hu, and Z. Wang, "A High-Efficiency Double DC-DC Conversion System for a Fuel Cell/Battery Hybrid Power Propulsion System in Long Cruising Range Underwater Vehicles," *Energy and Fuels*, vol. 34, no. 7, pp. 8872–8883, 2020, doi: 10.1021/acs.energyfuels.0c01287.
- [9] M. Voskuijl, J. van Bogaert, and A. G. Rao, "Analysis and design of hybrid electric regional turboprop aircraft," *CEAS Aeronaut. J.*, vol. 9, no. 1, pp. 15–25, Mar. 2018, doi: 10.1007/s13272-017-0272-1.
- [10] H. Gesell, F. Wolters, and M. Plohr, "System analysis of turbo-electric and hybrid-electric propulsion systems on a regional aircraft," *Aeronaut. J.*, vol. 123, no. 1268, pp. 1602–1617, 2019, doi: 10.1017/aer.2019.61.
- [11] M. Sielemann, D. Bermperis, J. Gohl, I. Torstensson, and K. Kyprianidis, "Benefit Reassessment of Parallel Hybrid Turboprops," 2023. doi: 10.2514/6.2023-4542.
- [12] A. Bills, S. Sripad, W. L. Fredericks, M. Singh, and V. Viswanathan, "Performance Metrics Required of Next- Generation Batteries to Electrify Commercial Aircraft," *ACS Energy Lett.*, vol. 5, no. 2, pp. 663–668, 2020, doi: 10.1021/acsenerylett.9b02574.
- [13] F. Afonso *et al.*, "Strategies towards a more sustainable aviation: A systematic review," *Prog. Aerosp. Sci.*, vol. 137, Feb. 2023, doi: 10.1016/j.paerosci.2022.100878.
- [14] D. Sziroczak, I. Jankovics, I. Gal, and D. Rohacs, "Conceptual design of small aircraft with hybrid-electric propulsion systems," *Energy*, vol. 204, Aug. 2020, doi: 10.1016/j.energy.2020.117937.
- [15] R. C. Bolam, Y. Vagapov, and A. Anuchin, "A Review of Electrical Motor Topologies for Aircraft Propulsion," *UPEC 2020 - 2020 55th Int. Univ. Power Eng. Conf. Proc.*, Sep. 2020, doi: 10.1109/UPEC49904.2020.9209783.
- [16] B. A. Adu-Gyamfi and C. Good, "Electric aviation: A review of concepts and enabling technologies," *Transp. Eng.*, vol. 9, Sep. 2022, doi: 10.1016/j.treng.2022.100134.
- [17] C. P. Nasoulis, V. G. Gkoutzamanis, and A. I.

- Kalfas, "Multidisciplinary conceptual design for a hybrid-electric commuter aircraft," *Aeronaut. J.*, vol. 126, no. 1302, pp. 1242–1264, 2022, doi: 10.1017/aer.2022.32.
- [18] T. Pattanayak and D. Mavris, "Battery technology for sustainable aviation: a review of current trends and future prospects," *Appl. Energy*, vol. 397, no. June, p. 126356, 2025, doi: 10.1016/j.apenergy.2025.126356.
- [19] B. J. Brelje and J. R. R. A. Martins, "Electric, hybrid, and turboelectric fixed-wing aircraft: A review of concepts, models, and design approaches," *Prog. Aerosp. Sci.*, vol. 104, no. August 2018, pp. 1–19, 2019, doi: 10.1016/j.paerosci.2018.06.004.
- [20] W. L. Fredericks, S. Sripad, G. C. Bower, and V. Viswanathan, "Performance Metrics Required of Next-Generation Batteries to Electrify Vertical Takeoff and Landing (VTOL) Aircraft," *ACS Energy Lett.*, vol. 3, no. 12, pp. 2989–2997, 2018, doi: 10.1021/acseenergylett.8b02195.
- [21] C. Pornet, S. Kaiser, A. T. Isikveren, and M. Hornung, "Integrated fuel-battery hybrid for a narrow-body sized transport aircraft," *Aircr. Eng. Aerosp. Technol.*, vol. 86, no. 6, pp. 568–574, Sep. 2014, doi: 10.1108/AEAT-05-2014-0062.
- [22] R. H. Jansen, C. Bowman, A. Jankovsky, R. Dyson, and J. Felder, "Overview of NASA electrified aircraft propulsion research for large subsonic transports," 2017. doi: 10.2514/6.2017-4701.
- [23] C. P. Nasoulis, G. Protopapadakis, E. G. Ntouvelos, V. G. Gkoutzamanis, and A. I. Kalfas, "Operating and Environmental Cost Considerations Comparison for Hybrid-Electric Propulsion Architecture Variants," *J. Phys. Conf. Ser.*, vol. 2526, no. 1, p. 012018, Jun. 2023, doi: 10.1088/1742-6596/2526/1/012018.
- [24] T. V. Marien *et al.*, "Results for an Electrified Aircraft Propulsion Design Exploration," 2021. doi: 10.23919/EATS52162.2021.9704848.
- [25] J. Goeing, L. Hanisch, S. Lück, M. Henke, and J. Friedrichs, "Modelling the nonlinear system performance of hybrid-electric propulsion systems with aerothermodynamic interdependencies," *J. Glob. Power Propuls. Soc.*, vol. 8, pp. 98–110, Apr. 2024, doi: 10.33737/JGPPS/186058.
- [26] S. Kang, I. Roumeliotis, J. Zhang, V. Pachidis, and O. Broca, "Assessment of Engine Operability and Overall Performance for Parallel Hybrid Electric Propulsion Systems for a Single-Aisle Aircraft," in *Proceedings of the ASME Turbo Expo*, Sep. 2021, vol. 4. doi: 10.1115/GT2021-58655.
- [27] M. Sielemann, J. Gohl, X. Zhao, K. Kyprianidis, G. Valente, and S. Sumsurooah, "On the Shaft Speed Selection of Parallel Hybrid Aero Engines," in *Proceedings of the ASME Turbo Expo*, Sep. 2021, vol. 1. doi: 10.1115/GT2021-59500.
- [28] T. Carpentier, J. Zhang, A. S. J. Van Heerden, and I. Roumeliotis, "Performance and Economic Assessment of Mechanically Integrated Parallel Hybrid Aircraft," in *Proceedings of the ASME Turbo Expo*, Oct. 2022, vol. 4. doi: 10.1115/GT2022-81939.
- [29] R. Ghelani *et al.*, "Design Methodology and Mission Assessment of Parallel Hybrid Electric Propulsion Systems," in *Proceedings of the ASME Turbo Expo*, Oct. 2022, vol. 1. doi: 10.1115/GT2022-82478.
- [30] S. Vouros, D. Hiebl, and K. Kyprianidis, "Impact of Boundary Layer Ingestion on the Performance of Propeller Systems for Hybrid Electric Aircraft," in *Proceedings of the ASME Turbo Expo*, Oct. 2022, vol. 1. doi: 10.1115/GT2022-82472.
- [31] S. Sahoo, M. D. Kavvalos, D. E. Diamantidou, and K. G. Kyprianidis, "System-Level Assessment of a Partially Distributed Hybrid Electric Propulsion System," in *Proceedings of the ASME Turbo Expo*, Oct. 2022, vol. 1. doi: 10.1115/GT2022-81917.
- [32] E. G. Engelbrecht, V. G. Gkoutzamanis, C. P. Nasoulis, and A. I. Kalfas, "Inlet Flow Distortion Dependencies for Tail Mounted Ducted Fans on Hybrid-Electric Commuter Aircraft," in *Proceedings of the ASME Turbo Expo*, Oct. 2022, vol. 1. doi: 10.1115/GT2022-80894.
- [33] F. R. Gimenez, C. E. K. Mady, and I. B. Henriques, "Assessment of different more-electric and hybrid-electric configurations for long-range multi-engine aircraft," *J. Clean. Prod.*, vol. 392, p. 136171, Mar. 2023, doi: 10.1016/J.JCLEPRO.2023.136171.
- [34] A. Boretti and S. Castelletto, "NH3 Prospects in Combustion Engines and Fuel Cells for Commercial Aviation by 2030," *ACS Energy Lett.*, vol. 7, no. 8, pp. 2557–2564, 2022, doi: 10.1021/acseenergylett.2c00994.
- [35] K. I. Papadopoulos, C. P. Nasoulis, V. G. Gkoutzamanis, and A. I. Kalfas, "Flight-Path Optimization for a Hybrid-Electric Aircraft," in *Proceedings of the ASME Turbo Expo*, Sep. 2023, vol. 5. doi: 10.1115/GT2023-103863.
- [36] R. Ghelani *et al.*, "Integrated Hybrid Engine Cycle Design and Power Management Optimization," Sep. 2023. doi: 10.1115/GT2023-103131.
- [37] T. Donato, A. Ficarella, and L. Spada Chiodo, "Dynamic Modeling and Degradation Study of a Hybrid Electric Power System for Urban Air Mobility," Sep. 2023. doi: 10.1115/GT2023-101597.
- [38] M. Fanxin, G. Zanjun, Z. Wenyuan, and H. Wenchao, "Research of key technologies for the

- more electrical aircraft electric cabin supply air system,” *IET Conf. Publ.*, vol. 2018, no. CP743, 2018, doi: 10.1049/cp.2018.0199.
- [39] Q. Zhu, A. Forsyth, and R. Todd, “Investigation of Hybrid Electric Aircraft Operation on Battery Degradation,” *2018 IEEE Int. Conf. Electr. Syst. Aircraft, Railw. Sh. Propuls. Road Veh. Int. Transp. Electrif. Conf. ESARS-ITEC 2018*, no. c, pp. 1–6, 2018, doi: 10.1109/ESARS-ITEC.2018.8607617.
- [40] A. Del Pizzo, L. P. Di Noia, and F. Marulo, “Design considerations on energy storage system for electric aircraft propulsion,” *AEIT 2016 - Int. Annu. Conf. Sustain. Dev. Mediterr. Area, Energy ICT Networks Futur.*, pp. 1–6, 2016, doi: 10.23919/AEIT.2016.7892786.
- [41] I. Hakyemez, O. Kagan Keles, O. Kalenderli, and M. Bagriyanik, “Conceptual Design of Modernized 270 VDC Electrical Power Distribution System for Hercules C-130 Aircraft,” *IEEE Access*, vol. 12, no. August, pp. 112053–112061, 2024, doi: 10.1109/ACCESS.2024.3443189.
- [42] C. Pernet and A. T. Isikveren, “Conceptual design of hybrid-electric transport aircraft,” *Prog. Aerosp. Sci.*, vol. 79, pp. 114–135, Nov. 2015, doi: 10.1016/J.PAEROSCI.2015.09.002.
- [43] S. Seyam, I. Dincer, and M. Agelin-chaab, “Investigation of Potential Fuels for Hybrid Molten Carbonate Fuel Cell-Based Aircraft Propulsion Systems,” *Energy and Fuels*, vol. 35, no. 12, pp. 10156–10168, 2021, doi: 10.1021/acs.energyfuels.1c00915.
- [44] G. Palaia and K. Abu Salem, “Mission Performance Analysis of Hybrid-Electric Regional Aircraft,” *Aerospace*, vol. 10, no. 3, 2023, doi: 10.3390/aerospace10030246.
- [45] V. O. Bonnin and M. F. M. Hoogreef, “Exploration of Off-Design Performance for Hybrid Electric Regional Aircraft,” *J. Aircr.*, vol. 62, no. 4, pp. 876–895, 2025, doi: 10.2514/1.C037893.
- [46] J. Kurzke, “GasTurb 12: Design and off-design performance of gas turbines.” GasTurb GmbH, Aachen, Germany, 2012.
- [47] EMBRAER, “A.P.120/731: Emb-120 Brasilia: Airport Planning Manual,” no. 4, Sao Jose dos Campos, p. 23, 2019. [Online]. Available: http://www.embraercommercialaviation.com/AMPS/APM_190
- [48] “Type-Certificate Data Sheet: Pw100 series engines - EASA.IM.E.041 - Pratt and Whitney Canada PW100 series engines,” Quebec, 2018. Accessed: Apr. 10, 2025. [Online]. Available: <https://www.easa.europa.eu/en/document-library/type-certificates/engine-cs-e/easaim041-pratt-and-whitney-canada-pw100-series>
- [49] P. P. Walsh and P. Fletcher, *Gas Turbine Performance*, 2nd ed. Oxford, UK: Wiley, 2004. doi: 10.1002/9780470774533.
- [50] C. Bringhenti, J. T. Tomita, and J. R. Barbosa, “Performance Study of a 1 MW Gas Turbine Using Variable Geometry Compressor and Turbine Blade Cooling,” in *Proceedings of the ASME Turbo Expo*, Dec. 2010, vol. 3, pp. 703–710. doi: 10.1115/GT2010-22867.
- [51] G. R. Matuck, J. R. Barbosa, C. Bringhenti, and I. Lima, “Gas Turbine Fault Detection and Isolation Using MLP Artificial Neural Network,” in *Proceedings of the ASME Turbo Expo*, Mar. 2009, vol. 1, pp. 803–811. doi: 10.1115/GT2007-27987.
- [52] “Type-Certificate Data Sheet: Engines-EASA.IM.E.038 - Pratt & Whitney Corp. PT6A-68 series engine,” Quebec, 2016. Accessed: Apr. 11, 2025. [Online]. Available: <https://www.easa.europa.eu/en/document-library/type-certificates/engine-cs-e/easaim038-pratt-whitney-corp-pt6a-68-series-engine>
- [53] J. L. F. and T. V. M. C. L. Bowman, “Turbo- and Hybrid-Electrified Aircraft Propulsion Concepts for Commercial Transport,” in *AIAA/IEEE Electric Aircraft Technologies Symposium (EATS)*, 2018, pp. 1–8. Accessed: Apr. 11, 2025. [Online]. Available: <https://ieeexplore.ieee.org/document/8552831>
- [54] J. Schömann, “Hybrid-Electric Propulsion Systems for Small Unmanned Aircraft,” Technische Universität München, Arcisstraße 21, 80333 München, Deutschland, 2013.
- [55] U. 09/2017-V03, “UNITEK: Digital three-phase servo amplifier: Bamocar-pg-d3,” Nellmersbach, Deutschland, 2017.
- [56] EMRAX, *Manual for EMRAX Motors / Generators*, no. March. Version 5.4. Slovenia, 2020. [Online]. Available: www.emrax.com
- [57] N. Harris McClamroch, *Steady aircraft flight and performance*. Princeton University Press, 2011.
- [58] G. Palaia, K. Abu Salem, and A. A. Quarta, “Parametric Analysis for Hybrid-Electric Regional Aircraft Conceptual Design and Development,” *Appl. Sci.*, vol. 13, no. 19, 2023, doi: 10.3390/app13191113.
- [59] J. D. . Anderson and C. Cadou, *Fundamentals of aerodynamics*, 7th ed. New York, NY: McGraw Hill LLC, 2024.
- [60] T. R. Yechout, S. L. Morris, D. E. Bossert, W. F. Hallgren, and J. K. Hall, *Introduction to Aircraft Flight Mechanics, Second Edition*, 2nd ed. Washington, DC: American Institute of Aeronautics and Astronautics, Inc., 2014. doi: 10.2514/4.102547.



GUSTAVO MULLER HAUCK

received the Engineering and M.S degrees in Aeronautical-Mechanical Engineering from Aeronautics Institute of Technology (ITA), Brazil, 2021 and 2023. He is currently an Officer in the Brazilian Air Force (FAB). He has experience in the field of Mechanical Engineering, with an emphasis on Aeronautical Propulsion.



MAURICIO ANDRÉS VARELA MORALES

received the title in Aeronautical Engineering from Aeronautics Institute of Technology in 2006, joined the University in 2009, and received his Master's (2010) and Doctorate (2016) degrees

in Aeronautical and Mechanical Engineering from the same institution. He is currently a Product Development Engineer at Embraer S.A., working in Flight Mechanics. He is also an Adjunct Professor in the Department of Flight Mechanics, Division of Aeronautical and Aerospace Engineering, at the Aeronautics Institute of Technology (ITA).



CLEVERSON BRINGHENTI is graduated in Physics from State University of Ponta Grossa (UEPG-PR) in 1996, received the Master and Doctoral degrees in Aeronautical and Mechanical Engineering in 1999 and 2003 from Aeronautics Institute of

Technology (ITA). He completed a Post-Doctoral at Aeronautics Institute of Technology (ITA) from 2003 to 2008 and received a degree in Industrial Mechanical Engineering, Escola Técnica Professor Everardo Passos, ETEP, in 2010. Cleverson worked at Brazilian Aeronautics Company, EMBRAER, from 2008 to 2009 in Market Intelligence. Since 2009 he has been a Professor in the Department of Turbomachines at Aeronautics Institute of Technology (ITA). Cleverson was Deputy Head of the Mechanical Engineering Division, Head of the Department of Turbomachines. He is currently Associate Professor IV, Head of the Mechanical Engineering Division. He has experience in the area of Mechanical-Aeronautical and Aerospace Engineering with an emphasis on Gas Turbines, Combined Cycle (Thermal Power Plants), Piston Engine and Propulsion. He is a reviewer at the Fundação de Amparo e Pesquisa do Estado de São Paulo (FAPESP), member of international committees (ASME-IGTI), coordinates and participates in research and development projects with

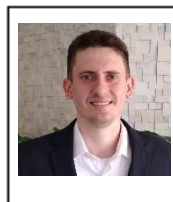
companies in the areas of Defense, Oil and Gas, generation of electrical and aeronautical energy.



JESUINO TAKACHI TOMITA

Graduated in Mechanical Engineering (Plena degree) from Faculdade de Engenharia Industrial – FEI (2000), with a master's (2003) and a Doctoral (2009) degrees in Aeronautical and

Mechanical Engineering from Aeronautics Institute of Technology (ITA) in the area of aerospace propulsion. Holds a C-Level Certification (Owners and Presidents Program / Top Management Program) from Insper and Columbia Business School (2023). Completed training in Corporate Governance and Board Development (2021) at the Instituto Euvaldo Lodi (IEL/FIEMG). Professor in the Department of Turbomachines, Division of Mechanical Engineering at ITA. He was Vice-Rector of ITA (2020–2024); Coordinator of the Mechanical-Aeronautical Engineering Program (2015–2017); Head of the Division of Continuing Education, Graduate School (2018–2020); Deputy Head of the Division of Mechanical Engineering (2018–2020); Head of the Department of Turbomachines (2014–2022); Member of the Aerospace Engineering Executive Committee (2011–2015) of the Brazilian Society of Mechanical Sciences and Engineering (ABCM); and Alternate Board Member of CREA-SP in the Specialized Chamber of Mechanical and Metallurgical Engineering (CEEMM), representing ITA (2011–2014), and was a Full Board Member in 2012. Currently serves as National Representative of the International Society of Air Breathing Engines (ISABE) since 2015 and as Member of the International Forum for Aviation Research (IFAR) in the Electric-Hybrid Propulsion area since 2023. Member of the American Society of Mechanical Engineers (ASME), participating in the Cycle Innovations and Education Committee.



ANTONIO BRUNO DE VASCONCELOS LEITÃO

Graduated in Mechanical Engineering from Federal University of Piauí (UFPI) (2015), and in Renewable Energies from UFPI (2025). Holds a Master's degree in Materials Science and Engineering from UFPI

(2016) and a Doctoral in Mechanical Engineering from the State University of Campinas (UNICAMP) (2020). He has professional and research experience in Mechanical Engineering. Currently He is a Post-Doctoral at Aeronautics Institute of Technology (ITA).



FRANCO JEFFERDS DOS SANTOS SILVA is Adjunct Professor in Turbomachinery Department at Mechanical Engineering Division from Aeronautics Institute of Technology (ITA). He received a Master and

Doctoral in Aeronautical and Mechanical Engineering from Aeronautics Institute of Technology (ITA), his master and doctoral researches focused on gas turbines performance under the influence of variable geometry transients, a critical field for the aerospace and energy industry. In addition to his academic background, he has professional experience, including a position as a Senior Mechanical Engineer at Vale Mining Company (2011-2014), where he played a significant role in the mine equipment maintenance engineering team. In academia. He was the Course Coordinator in the Faculty of Mechanical Engineering (2014-2016 - Universidade Federal do Sul e Sudeste do Pará - UNIFESSPA), Coordinator of the Intellectual Property and Technology Transfer Postgraduate Program for Innovation - Profnit (2018-2019, Universidade Federal do Sul e Sudeste do Pará - UNIFESSPA), Head of the Technological Innovation Division (2016-2020, Universidade Federal do

Sul e Sudeste do Pará - UNIFESSPA), Director of Research and Technological Innovation at the Office of Postgraduate Studies, Research, and Technological Innovation (2020-2021, Unifesspa), and Director of the Faculty of Mechanical Engineering (2022-2023, Universidade Federal do Sul e Sudeste do Pará - UNIFESSPA).



KONSTANTINOS KYPRIANIDIS is Professor at School of Business Society and Engineering, Division of Sustainable Energy Systems at Mälardalen University, Västerås, Sweden. He is a Full Professor in Energy Engineering and drive research

primarily within the field of digitalization and automation. Application domains include aerospace, power generation, process and manufacturing industry. He is also the Director of Research Education in Engineering (EST). He holds a PhD in Gas Turbine Engineering from Cranfield University (2010) -and a Dipl-Ing in Mechanical Engineering from Aristotle University of Thessaloniki (2006). He received a second PhD in Gas Turbine Engineering from Cranfield University.